frontiers in Earth Science

ORIGINAL RESEARCH
published: 25 February 2021
doi: 10.3389/feart.2021.591948

Atmospheric and Oceanographic Forcing Impact Particle Flux Composition and Carbon Sequestration in the Eastern Mediterranean Sea: A Three-Year Time-Series Study in the Deep Ierapetra Basin

Rut Pedrosa-Pamies[1,2], Constantine Parinos[3], Anna Sanchez-Vidal[2], Antoni Calafat[2], Miquel Canals[2], Dimitris Velaoras[3], Nikolaos Mihalopoulos[4,5], Maria Kanakidou[4], Nikolaos Lampadariou[3] and Alexandra Gogou[3]*

[1]*The Ecosystems Center, Marine Biological Laboratory, Woods Hole, MA, United States,* [2]*Consolidate Research Group in Marine Geosciences, Department of Earth and Ocean Dynamics, Faculty of Earth Sciences, University of Barcelona, Barcelona, Spain,* [3]*Institute of Oceanography, Hellenic Centre for Marine Research (HCMR), Anavyssos, Greece,* [4]*Environmental Chemical Processes Laboratory (ECPL), Department of Chemistry, University of Crete, Heraklion, Greece,* [5]*Institute for Environmental Research and Sustainable Development (IERSD), National Observatory of Athens, Athens, Greece*

OPEN ACCESS

Edited by:
Timothy Ferdelman, Max Planck Institute for Marine Microbiology (MPG), Germany

Reviewed by:
Gerard Versteegh, Alfred Wegener Institute Helmholtz Center for Polar and Marine Research (AWI), Germany
Facundo Matias Barrera, University of Concepción, Chile

***Correspondence:**
Rut Pedrosa-Pamies
rpedrosa@mbl.edu

Specialty section:
This article was submitted to Biogeoscience, a section of the journal Frontiers in Earth Science

Received: *05 August 2020*
Accepted: *06 January 2021*
Published: *25 February 2021*

Citation:
Pedrosa-Pamies R, Parinos C, Sanchez-Vidal A, Calafat A, Canals M, Velaoras D, Mihalopoulos N, Kanakidou M, Lampadariou N and Gogou A (2021) Atmospheric and Oceanographic Forcing Impact Particle Flux Composition and Carbon Sequestration in the Eastern Mediterranean Sea: A Three-Year Time-Series Study in the Deep Ierapetra Basin. Front. Earth Sci. 9:591948. doi: 10.3389/feart.2021.591948

Sinking particles are a critical conduit for the export of organic material from surface waters to the deep ocean. Despite their importance in oceanic carbon cycling, little is known about the biotic composition and seasonal variability of sinking particles reaching abyssal depths. Herein, sinking particle flux data, collected in the deep Ierapetra Basin for a three-year period (June 2010 to June 2013), have been examined at the light of atmospheric and oceanographic parameters and main mass components (lithogenic, opal, carbonates, nitrogen, and organic carbon), stable isotopes of particulate organic carbon (POC) and source-specific lipid biomarkers. Our aim is to improve the current understanding of the dynamics of particle fluxes and the linkages between atmospheric dynamics and ocean biogeochemistry shaping the export of organic matter in the deep Eastern Mediterranean Sea. Overall, particle fluxes showed seasonality and interannual variability over the studied period. POC fluxes peaked in spring April–May 2012 (12.2 mg m^{-2} d^{-1}) related with extreme atmospheric forcing. Summer export was approximately fourfold higher than mean wintertime, fall and springtime (except for the episodic event of spring 2012), fueling efficient organic carbon sequestration. Lipid biomarkers indicate a high relative contribution of natural and anthropogenic, marine- and land-derived POC during both spring (April–May) and summer (June–July) reaching the deep-sea floor. Moreover, our results highlight that both seasonal and episodic pulses are crucial for POC export, while the coupling of extreme weather events and atmospheric deposition can trigger the influx of both marine labile carbon and anthropogenic compounds to the deep Levantine Sea. Finally, the comparison of time series data of sinking particulate flux with the corresponding

biogeochemical parameters data previously reported for surface sediment samples from the deep-sea shed light on the benthic–pelagic coupling in the study area. Thus, this study underscores that accounting the seasonal and episodic pulses of organic carbon into the deep sea is critical in modeling the depth and intensity of natural and anthropogenic POC sequestration, and for a better understanding of the global carbon cycle.

Keywords: sinking particle fluxes, carbon cycle, lipid biomarkers, atmospheric forcing, eastern mediterranean sea, surface sediment, deep ocean, particulate organic carbon

INTRODUCTION

The export of carbon from the surface to the deep ocean through sinking particulate biogenic material, also known as the biological pump (Volk and Hoffert, 1985), is an essential component of the ocean carbon cycle. This plays an important role in atmospheric CO_2 fluctuations (Archer et al., 2000; Kwon et al., 2009; Lima et al., 2014) and in deep ocean ecosystems functioning (Smith et al., 2009 and references therein). The overall fraction of net primary production (NPP) that is exported from the surface ocean to the mesopelagic and bathypelagic layers and the vertical attenuation of this flux with depth are both good measures of the export efficiency (POC export flux/NPP) of the biological pump (De La Rocha and Passow, 2007; DeVries et al., 2012), which is largely being determined by the structure and functioning of the ocean's ecosystem (e.g., Francois et al., 2002; Honjo et al., 2008; Dagg et al., 2014; Le Moigne et al., 2016). However, the processes controlling the biological pump efficiency are not fully understood (Boyd and Trull, 2007). Since oligotrophic waters cover about 75% of the ocean surface (Lewis et al., 1986) and contribute over 30% of the global marine carbon fixation (Longhurst et al., 1995; Marañón et al., 2003), understanding these processes therein is critical in order to assess their biogeochemical functioning and feedbacks between the ocean carbon cycle and human-induced environmental change.

The Eastern Mediterranean Sea (EMS) is one of the most oligotrophic areas of the world ocean, in other words "an oceanic desert" (Azov, 1991). It exhibits ultra-oligotrophic characteristics, related to: 1) a net outflow of nutrients due to its anti-estuarine circulation, 2) nutrient-depleted surface Atlantic Water flowing in through the Strait of Sicily and nutrient-rich Levantine Intermediate Water flowing out at intermediate depths (Ribera d'Alcalà, 2003; Huertas et al., 2012), and 3) extremely low phosphorus levels, which strongly limits both primary and secondary productions (Krom et al., 1991). Carbon vertical flux was found to be differentiated along a north-south oligotrophy gradient and "hot spots" for CO_2 sequestration to the ocean interior on long time scales were detected in the less oligotrophic area (Siokou-Frangou et al., 2002; Gogou et al., 2014; Pedrosa-Pàmies et al., 2016; Pavlidou et al., 2020). The weak seasonality of the phytoplankton biomass and production drives NPP rates below 200 mg C m^{-2} d^{-1} (Psarra et al., 2000; Moutin and Raimbault, 2002; Bosc, 2004), while very low amounts of POC (<0.5% of NPP) reach the deep sea floor (Warnken, 2003; Koppelmann et al., 2004; Stavrakakis et al., 2013; Gogou et al., 2014; Pedrosa-Pàmies et al., 2016; Karageorgis et al., 2018).

The oligotrophic regime of the EMS is modulated by sub-basin gyres and mesoscale features. These may result in distinct changes of the water column biogeochemical properties, through the horizontal and vertical mass transfer that play an important role on nutrient and carbon distribution (Siokou-Frangou et al., 2010, and references therein). Moreover, in the EMS atmospheric deposition plays a major role in the supply of bioavailable nutrients and anthropogenic compounds due to the limited inputs from external sources (Krom et al., 2004; Christodoulaki et al., 2013; Theodosi et al., 2019; Kanakidou et al., 2020). A variety of sources at the regions surrounding the Mediterranean Sea, but also distant sources due to long range transport of air masses, affect the quality of atmospheric deposition which could have important implications on the pelagic productivity and, overall, carbon cycle (Kouvarakis et al., 2001; Jickells et al., 2005; Kanakidou et al., 2012).

Understanding the processes that control the quantity and quality of POC flux to the deep EMS is needed to better characterize the strength and efficiency of the biological pump as well as to accurately project the response of this oligotrophic system to climate fluctuations and anthropogenic perturbations. Bulk geochemical proxies, such as the stable isotopic composition of organic carbon ($\delta^{13}C$), and lipid biomarkers have been widely used as indices of sources and transformation processes of organic matter in marine systems (Meyers, 1994; Wakeham, 1995; Volkman and Tanoue, 2002; Goñi et al., 2003; Hu et al., 2006; Pedrosa-Pàmies et al., 2013; Quirós-Collazos et al., 2017), as well as to assess the biogeochemical dynamics controlling the export of POC to the deep sea (Goutx et al., 2000; Wakeham et al., 2002; Conte et al., 2003; Pedrosa-Pàmies et al., 2018, 2019; De Bar et al., 2019). While there have been several investigations on the $\delta^{13}C$ signature of sinking particles in the Mediterranean Sea (Kerhervé et al., 2001; Turchetto et al., 2012; Pasqual et al., 2015; Theodosi et al., 2019) but also on the molecular composition of POC particulate fluxes in the western Mediterranean Sea, both in the upper mesopelagic layers (100–300 m depth) (e.g., Tolosa et al., 2005; Goutx et al., 2007; Marty et al., 2009; Méjanelle and Dachs, 2009) and the deep sea (Marchand et al., 2005; Wakeham et al., 2009), little is known about the POC molecular composition of the EMS particle fluxes (Tsapakis et al., 2006; Theodosi et al., 2013) and deep-sea floor (Gogou and Stephanou, 2004; Parinos et al., 2013a; Pedrosa-Pàmies et al., 2015).

Herein, we present a 3-year time series of sinking particles flux data in the deep Ierapetra Basin (4,310 m depth). The collected data have been examined at the light of atmospheric and oceanographic parameters and main mass components (lithogenic, calcium carbonate, opal and organic matter), stable isotopic composition of POC and source-specific

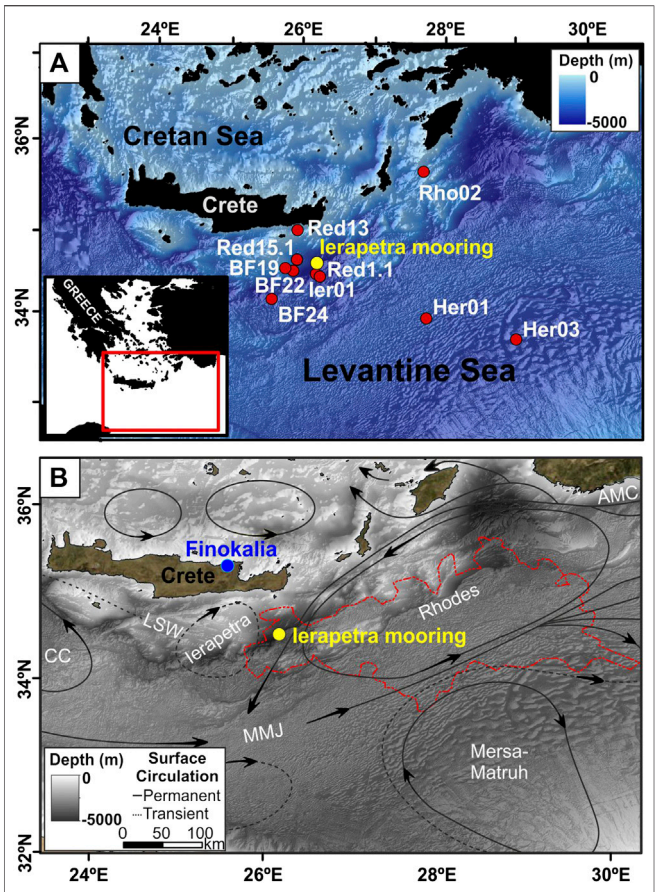

FIGURE 1 | (A) Location of the mooring line deployed in the deep Ierapetra Basin from June 2010 to June 2013 (yellow dot), and 10 surface sediment samples collected in the Levantine Sea (red dots) reported by Pedrosa-Pàmies et al. (2015) (lipid data for sediment samples BF19, BF22 and BF24 are not available). **(B)** Schematic representation of the upper thermocline circulation in the study area (Robinson and Golnaraghi, 1993), and location of Ierapetra mooring (yellow dot), and Finokalia atmospheric station (blue dot). Circulation patterns and water masses: MMJ-Mid-Mediterranean Jet, AMC-Asia Minor Current, LSW-Levantine Surface Water, CC-Cretan Cyclone. The dashed red polygon is the contour of the Rhodes Gyre phytoplankton bloom of March 2012 as indicated by Chlorophyll-*a* concentrations above 0.2 mg m^{-3} (48291.3 km^2). The bathymetric map was produced using metadata from the EMODnet Bathymetry portal—http://www.emodnet-bathymetry.eu.

lipid biomarkers (long chain *n*-alkanes and the unresolved complex mixture of aliphatic hydrocarbons, long-chain *n*-alkanols, long-chain alkenones, long-chain diols&keto-ols and selected sterols). The aim of the present study is to improve the current understanding of the dynamics of particle fluxes and the linkages between atmosphere dynamics and ocean biogeochemistry shaping the export of organic matter in this oligotrophic abyssal region of the EMS. Moreover, in order to evaluate the benthic-pelagic coupling in the study area, the time series of sinking particles flux data were compared to the corresponding data of biogeochemical parameters previously reported for surface sediments from the deep-sea in the study area. To the best of our knowledge, this study presents for the first time the lipid biomarker composition of sinking particles reaching the deep EMS.

OCEANOGRAPHIC AND ATMOSPHERIC SETTINGS

The northwestern part of the Levantine Basin covers an area extending from south of Crete up to the southeast of Rhodes island. It is dominated by the presence of the permanent Rhodes cyclonic gyre centered south of Rhodes but occasionally expanding westwards toward Crete (**Figure 1**). A second feature is the recurrent Ierapetra anticyclonic gyre situated to the southeast of Crete (Larnicol et al., 2002; Mkhinini et al., 2014) showing a climatological mean position close to 26–27°E and 34–35°N. The Ierapetra anticyclone is a mesoscale eddy created by the strong northerly Etesian winds and their interaction with the orography of the island of Crete. Its seasonal variability relates to that of the Etesians, hence it starts developing in summer and intensifies in autumn. Its seasonal variability is correlated with an average three-month lag between maximum negative wind stress curl caused by the Etesians and maximum negative current vorticity linked to the anticyclone (Amitai et al., 2010). The Ierapetra anticyclone entraps water masses exiting from the Cretan straits enhancing the downward fluxes/transport of particulate matter and nutrient-depleted waters with important implications on the biogeochemical functioning of the area (Lampadariou et al., 2009; Pedrosa-Pàmies et al., 2015). The Ierapetra anticyclone also presents interannual variability in intensity and positioning. Nevertheless, during the study period (2010–2013) it had rather typical seasonal behavior (Ioannou et al., 2017).

The Levantine Basin atmosphere is at the crossroad of air masses of various origins that affect atmospheric composition. Air masses coming from the south carry significant amounts of African desert dust, from the northwest/north/northeast carry anthropogenic pollution from Central Europe, Balkans, and Ukraine, and Turkey, respectively from the east air masses are rich in dust mixed with anthropogenic pollution from the Middle-East, while coming from the west air masses are significantly affected by marine emissions (Kanakidou et al., 2011). In addition, when passing over continental regions, air masses are also affected by land sources (i.e., vegetation, forest fires, soil resuspension) (Sciare et al., 2003), and are enriched in air pollutants emitted by land sources (Mihalopoulos et al., 1997; Lelieveld et al., 2002; Kanakidou et al., 2011). Therefore, the quality of atmospheric deposition and its fingerprint in the export of material in the seawater column depend upon the origin of the air masses that are reaching the area during the study period.

METHODS AND DATA

Oceanographic and Atmospheric Data

To investigate the effects of various atmospheric and upper ocean processes on particle fluxes, we consider a variety of environmental parameters for the study area during the investigated period, i.e.

atmospheric deposition, sea surface temperature (SST), surface Chlorophyll *a* (Chl *a*) concentration, and net primary production (NPP). These data were obtained either from *in-situ* observations or satellite data from one grid cell above the location of the sediment trap: 34.3–34.6°N, 26.0–26.3°E (see below for details).

Total atmospheric deposition data (dry and wet deposition) were obtained from the Finokalia atmospheric monitoring station located at a remote site in the northern coast of the island of Crete, Greece (35°20′N, 25°40′E; **Figure 1**). The site is not impacted by local human activities and it is a well characterized location for atmospheric composition and deposition, characteristic for the eastern Mediterranean atmosphere, operating since 1993 (Mihalopoulos et al., 1997). Moreover, in order to investigate the potential sources that contributed to the atmospheric deposition and therefore affected the flux of material into the sea water column during the study period, characteristic air mass 5-days back-trajectories have been calculated and analyzed. The back-trajectories have been computed using the HYSPLIT trajectory model of NOAA (Stein et al., 2015; Rolph et al., 2017) and considering as arriving point the Finokalia atmospheric monitoring station at 1,000 and 3,000 m.

Monthly SST and 8-days Chl *a* concentrations were obtained from the Moderate Resolution Imaging Spectrometer (MODIS), in orbit on the Aqua platform, using 4-km resolution level 3-binned data. Both monthly SST and Chl *a* data are processed and distributed by the NASA Goddard Earth Sciences (GES) Data, Information Services Center (DISC) and Ocean Biology Processing Group (OBPG). Monthly NPP estimates (1/12° resolution) were obtained from the Vertically Generalized Production Model (VGPM) (Behrenfeld and Falkowski, 1997), and provided by the Oregon State University (OSU).

Additionally, deep-sea daily mean current speed and direction at the deep Ierapetra Basin were evaluated. The moored line deployed in the Ierapetra Basin, included an Aanderaa RCM8 current meter deployed at 23 m above the bottom with a measuring interval of 1 h.

Sample Collection

Sinking particles were collected at 4,285 m water depth with a PPS3 Technicap sequential sampling sediment trap (0.125 m^2 collecting area) from June 2010 to June 2013 at the 4,310 m deep Ierapetra Basin (**Figure 1**). The trap was equipped with 12 receiving cups with a sampling interval of 1 month. The collecting cups were filled with a 5% (*v/v*) formaldehyde solution in 0.45 μm filtered seawater buffered with sodium borate. As earlier reported by Altabet (2001), formaldehyde preservative does not add sufficient organic carbon to the sediment trap material to alter organic composition (e.g., $\delta^{13}C$ of POC), and it has been extensively used for the preservation of sediment trap material (Thunell et al., 2000; Tolosa et al., 2003; Struck et al., 2004; Sanchez-Vidal et al., 2008; Tesi et al., 2010; Henley et al., 2012). After recovering, sediment trap samples were stored in the dark at 2–4°C until they were further processed in the laboratory.

Moreover, in order to evaluate the benthic-pelagic linkages in the study area, the time series data of sinking particles flux are being discussed along with the corresponding biogeochemical parameters and lipid compounds/indices data previously reported by Pedrosa-Pàmies et al. (2015) for surface sediment samples (undisturbed top 0–1 cm) collected from January 2007 to June 2012 in the NW Levantine Sea (**Figure 1**, **Supplementary Table S1**). The sedimentation rate in the deep EMS is in the order of 0.003 cm y^{-1} (Van Santvoort et al., 1996).

Analytical Methods

Elemental and Stable Isotope Analysis of Carbon

Sediment trap samples were processed in the laboratory according to a modified version of Heussner et al. (1990). Large swimming organisms were removed by wet sieving through a 1 mm nylon mesh, while organisms <1 mm were handpicked under a microscope with fine tweezers. Samples were repeatedly split into aliquots using a high precision peristaltic pump robot to obtain 10–20 mg subsamples, and then they were stirred three times with ultrapure water, centrifuged and the supernatant removed to eliminate salt and formaldehyde. Samples were finally freeze-dried and weighted for total mass determination.

Total carbon (TC), POC and total nitrogen (TN) contents and stable isotopic composition of POC were analyzed using a Flash 1112 EA elemental analyzer interfaced to a Delta C Finnigan MAT isotope ratio mass spectrometer. Samples analyzed for %OC and $\delta^{13}C$ were initially de-carbonated using repetitive additions of a 25% HCl (*v/v*) solution, separated by 60°C drying steps, until no effervescence was observed (Nieuwenhuize et al., 1994). Uncertainties for elemental composition were lower than 0.1%, while uncertainty for $\delta^{13}C$ was lower than 0.05‰. In consistency with published data in the Mediterranean Sea we assumed OM as twice the OC content (e.g., Heussner et al., 1996; Masqué et al., 2003). The inorganic carbon content was calculated from the difference between TC and OC measurements. Assuming all inorganic carbon is contained within calcium carbonate, $CaCO_3$ content was determined using the molecular mass ratio of 100/12 [(TC%−OC%)×8.33].

Molar TN/POC ratios were also calculated. TN/POC is plotted in order to constrain the elemental ratios of N-depleted samples (i.e. TN/POC ≈0 rather than POC/TN ∞ 0) following Goñi et al. (2006), and to avoid the underestimation of the terrestrial-derived carbon fraction (Perdue and Koprivnjak, 2007).

Biogenic Opal and Lithogenic Fraction Analysis

The biogenic silica content was analyzed using a two-step 2.5 h extraction with a 0.5 M Na_2CO_3 solution, separated by centrifugation of the leachates. Si and Al contents of both leachates were analyzed with a Perkin-Elmer Optima 3200RL Inductive Coupled Plasma Optical Emission Spectrometer (ICP-OES), correcting the Si content of the first leachate by the Si/Al ratio of the second one (Kamatani and Oku, 2000). All values are reported as opal ($SiO_2.0.4H_2O$), a parameter defined by 2.4 times the weight percentage of biogenic Si content determined for each sample (Mortlock and Froelich, 1989). The opal detection limit, associated to the detection limit of the ICP-OES system, is approximately 0.2%. Analytical precision of opal measurements was 4.5%.

The lithogenic fraction was estimated by subtracting the concentration of the major constituents from total dry weight [%lithogenic = 100 – (%OM + %$CaCO_3$ + %opal)]. This fraction represents the residual component of particles such as quartz, feldspars, clay minerals and aluminosilicates (Mortlock and Froelich, 1989).

Lipid Biomarkers

A range of selected lipid biomarkers are considered in this study, namely long chain *n*-alkanes and the unresolved complex mixture of aliphatic hydrocarbons, long-chain *n*-alkanols, long-chain di- and tri-unsaturated C_{37} and C_{38} methyl ketones and C_{38} ethyl ketones, commonly referred to as long-chain alkenones, long-chain diols and keto-ols and a suite of sterols.

The analytical procedure followed for the determination of lipid biomarkers has been previously presented in detail (Gogou et al., 1998, 2000, 2007). Briefly, freeze-dried samples were initially solvent-extracted three times by sonication with dichloromethane. Combined extracts were subsequently separated into different compound classes by column chromatography using silica gel that had been activated for 1 h at 150 °C. The following solvent systems were used to elute the different compound classes of the considered lipid compounds: (1) *n*-hexane (fraction F1; aliphatic hydrocarbons), (2) dichloromethane/*n*-hexane (fraction F2; long-chain alkenones) and (3) ethyl acetate/*n*-hexane (fraction F3; *n*-alkanols, sterols, diols and keto-ols).

F1 and F3 fractions were analyzed by Gas Chromatography-Mass Spectrometry (GC-MS) while F2 fractions were analyzed by Gas Chromatography using Flame Ionization Detection (GC-FID). Hydroxyl-bearing compounds (fraction F3) were derivatized to the corresponding trimethylsilyl ethers prior to GC-MS analysis using N,O-bis-(trimethylsilyl)-trifluoroacetamide (BSTFA) + 1% trimethylchlorosilane (TMCS) for 1 h at 90 °C. Details regarding the GC instrumental parameters are presented elsewhere (Gogou et al., 2007; Parinos et al., 2013a).

The individual lipids were identified by a combination of comparison of GC-retention times to authentic standards and comparison of their mass spectral data to those in the literature. Quantification was based on the GC-MS or GC-FID response and comparison of peak areas with those of known quantities of standards added prior to the extraction of the samples ([$^2H_{50}$] *n*-tetracosane for *n*-alkanes, *n*-hexatriacontane for long-chain alkenones, 5α-androstan-3β-ol for sterols, diols and keto-ols, and *n*-heneicosanol for *n*-alkanols).

Source Indicators of Sinking Particulate Organic Carbon

The study of the natural isotopic variations of organic carbon ($\delta^{13}C$) is a valuable tool to trace sources and transformation processes of the particulate organic matter in the marine environment. The isotopic variations of carbon in the organic particles initially present depletion in ^{13}C, which derives from the formation procedures of the organic matter during primary production (Kerhervé et al., 2001). Then, a stepwise enrichment of ^{13}C occurs in the particles through the food chain and by the processes that are performed at the successive trophic levels (Altabet, 1996). According to this, the isotopic ratios of carbon, should be essentially affected both by the biological sources of the particles and the transformation processes that the latter have to undergo during their transfer through the water column (Kerhervé et al., 2001).

Concerning the suite of lipid biomarkers employed in this study, they have been widely used as proxies to identify the relative importance of natural *vs* anthropogenic, marine- and land-derived, sources for settling particulate matter along with the food web dynamics in the overlying water column (Meyers, 1997; Volkman, 2006; Christodoulou et al., 2009; Close et al., 2014; Pedrosa-Pàmies et al., 2015, 2019).

Herein, the sum of the concentrations of the considered lipid biomarkers having a marine (algal) origin was calculated as follows:

$$\sum \text{Phyto} = \sum (28\Delta^{5,22E} + 4\alpha C_{30}\Delta^{22E} + C_{30}\ \text{diols\&keto-ols} + \text{alkenones}) \quad (1)$$

where $C_{28}\Delta^{5,22E}$ is brassicasterol (24-methyl cholest-5,22-dien-3β-ol), and $4\alpha C_{30}\Delta^{22E}$ is dinosterol (4α,23,24R-trimethyl-5α-cholest-22-en-3β-ol).

Brassicasterol ($C_{28}\Delta^{5,22E}$) is primarily derived from diatoms and *Prymnesiophyta*, while dinosterol ($4\alpha C_{30}\Delta^{22E}$) is a major compound in many dinoflagellates (Volkman, 1986). Long-chain alkenones are produced by some *Prymnesiophyte* class, e.g., *Emiliania huxleyii* (Marlowe et al., 1984) the later constituting the dominant primary producers across the Mediterranean Sea (Ziveri et al., 2000; Triantaphyllou, 2004; Skampa et al., 2019). Long-chain C_{30} *n*-alkan-1,15-diols have been commonly reported in marine and freshwater environments (Versteegh et al., 1997, 2000; Rampen et al., 2012; Pedrosa-Pàmies et al., 2015, 2018, 2019), but little is known about their specific biological sources. They have been identified in the microalgae *Nannochloropsis* sp (class Eustigmatophyceae) (Volkman, 1986; Volkman et al., 1992; Gelin et al., 1997; Versteegh et al., 1997). C_{30} keto-ols might result from oxidation of the corresponding C_{30} diols (Volkman, 1986; Volkman et al., 1999; Rampen et al., 2012), or, on the contrary, as recently suggested by Versteegh and Lipp (2019), might be produced by currently uncharacterized source organisms.

In addition, we have evaluated the abundance of both cholesterol and β-sitosterol. Cholesterol ($C_{27}\Delta^5$, cholest-5-en-3β-ol) is ubiquitous in the marine environment, both in plants and animals (e.g., Harvey et al., 1989; Volkman et al., 1992, 1999). However, high concentrations cholesterol is typically associated with the existence of marine consumers such as zooplankton and benthic animals (Teshima, 1971; Volkman, 1986; Harvey et al., 1989; Grice et al., 1998), and fecal material (Prahl et al., 1984; Neal et al., 1986; Wakeham and Canuel, 1986). β-Sitosterol ($C_{29}\Delta^5$, 24-Ethylcholest-5-en-3β-ol) may derive from both terrigenous and marine sources (Volkman, 1986).

The abundance of the Unresolved Complex Mixture (UCM) of aliphatic hydrocarbons, a commonly observed persistent contaminant mixture in environmental samples consisting of

branched alicyclic hydrocarbons (Gough and Rowland, 1990), is used as an indicator of the contribution of anthropogenic organic matter from degraded petroleum hydrocarbons and/or apolar products deriving from combustion processes, such as grass/wood/coal combustion and/or the incomplete combustion of fossil fuels (e.g., Simoneit, 1984; Wang et al., 1999; Hays, 2004 and references therein).

The carbon preference index of long-chain *n*-alkanes (C*n* with $n \geq 25$; CPI_{NA}) refers to the ratio of the concentrations of the long straight-chain homologues with an odd number of carbon atoms over those with an even number of carbon atoms. Higher (terrestrial) plants produce a higher proportion of odd than even hydrocarbons with a CPI_{NA} of ≥4 (Eglinton and Hamilton, 1967; Collister et al., 1994). Fossil fuels have a CPI_{NA} of ~1 (Wang et al., 1999). For phytoplankton, data are not conclusive, though they generally tend to produce shorter *n*-alkanes (C*n* with $n < 20$) (Volkman et al., 1998). The index is calculated as:

$$CPI_{NA} = \sum([n-C_{25}] - [n-C_{33}])/\sum([n-C_{26}] - [n-C_{34}]) \quad (2)$$

The sum of the concentrations of the most abundant high molecular weight odd *n*-alkanes (TerNA) and even *n*-alkanols (TerN-OH), which are major components of epicuticular higher plant waxes (Eglinton and Hamilton, 1967; Ohkouchi et al., 1997), are defined, respectively, as:

$$\sum \text{TerNA} = \sum n-C_{27,29,31,33} \quad (3)$$

$$\sum \text{TerN-OH} = \sum n-C_{24,26,28,30} \quad (4)$$

With their total sum referred to hereafter as ∑Ter:

$$\sum \text{Ter} = \sum \text{TerNA} + \sum \text{TerN-OH} \quad (5)$$

Since the CPI_{NA} values are indicative of a mixture of both fossil and land-derived long-chain *n*-alkanes in most of the cases (see discussion below), the *n*-alkane contribution by fossil fuels ($CPI_{NA} = 1$) was subtracted in order to obtain the distribution signatures of the plant wax *n*-alkanes. To this, each individual terrestrial higher plant wax *n*-alkane signature considered in ∑TerNA sum was calculated by subtracting the average of the next higher and lower even carbon numbered homolog after Schneider et al. (1983), Simoneit et al. (1990) and Aboul-Kassim and Simoneit (1995) as follows:

$$\text{Wax } n-C_n = [C_n] - 0.5[C_{(n+l)} - C_{(n-1)}] \quad (6)$$

Statistical Analysis

Principal component analysis (PCA) (Meglen, 1992) was performed to identify the dominant factors of the variance within the dataset. Several studies have successfully applied PCA for discriminating organic matter sources (Reemtsma and Ittekkot, 1992; Yunker et al., 1995; Goñi et al., 2000; Pedrosa-Pàmies et al., 2015, 2019) and its transformation patterns in marine systems (Dauwe and Middelburg, 1998; Sheridan et al., 2002; Pedrosa-Pàmies et al., 2018). The observations include 30 sediment trap samples collected during the study period. Samples RedI-3 and RedI-6 are excluded due to lack of atmospheric deposition data for those months, RedII-8 and RedII-9 (Jan–Feb. 2012) and RedIII-4 (Sep. 2012) due to no data for lipids are available, and Red III-11 (Apr. 2013) due to it is an outlier based on the interquartile range of cholesterol (see "**Lipid Biomarkers**" section). The 18 variables considered refer to environmental conditions (SST, NPP, total atmospheric deposition), bulk properties (fluxes of POC, TN, $CaCO_3$, lithogenic, TN/POC ratio, and $\delta^{13}C$) and lipid biomarkers (fluxes of ∑TerNA, ∑TerN-OH, UCM, cholesterol, brassicasterol, β-sitosterol, dinosterol, C_{30}diol&keto-ols, and CPI_{NA}).

Prior to PCA, the data were standardized using the mean values and standard deviations to bring all of the variables into proportion with one another. A subroutine, the Varimax rotation, was applied to the first three factors in order to maximize or minimize loadings within each factor and thus simplify the visual interpretation of PCA projections. Correlation analysis was also performed using the same variables. PCA was carried out by using STATGRAPHICS v. 18.

RESULTS

Environmental Conditions

Total atmospheric deposition ranged from 130 to 5,600 mg m^{-2} $month^{-1}$ (**Figure 2A**). Highest atmospheric wet deposition was recorded in winter, especially in Feb 2011. Highest dry deposition was recorded in summer (Jul 2011), early fall (Sep 2011), and spring (Apr 2013). SST was highest during summer (25.5 ± 1.85°C) and lowest during winter (17.9 ± 1.69°C) (**Figure 2A**). Total Chl *a* concentrations were lowest during summer (0.07 ± 0.01 mg m^{-3}), relatively high during winter-spring (0.14 ± 0.05 mg m^{-3}), and the highest in March 2012 (0.43 mg m^{-3}). NPP followed the same trends as Chl *a* concentrations, with highest values in March 2012 (696 mg C m^{-2} d^{-1}) (**Figure 2B**).

Deep-sea currents at the sediment trap site at in the deep Ierapetra Basin were extremely slow with a predominant S/SW direction of the flow (**Figure 2C**). Intensified current speeds were recorded in January 2011 (up to 8 cm s^{-1}) and March 2012 (up to 9.8 cm s^{-1}) with a SW direction (i.e., topographically constrained). The magnitude of the current speeds and the strong topographic control registered in the deep Ierapetra Basin are of the same magnitude as currents registered at 3,542 m in the Samaria Canyon at the southern Cretan margin (Karageorgis et al., 2018) and at 4,300 m at NESTOR site in the deep Ionian Sea (Stavrakakis et al., 2013).

Sinking Particle Fluxes and Component Ratios

Total mass flux (TMF) and its major constituents (organic matter, opal, $CaCO_3$, and lithogenic matter) were highly variable, including significant seasonal variations (**Figure 3**, **Table 1**). During the three-year deployment, TMF ranged from 1.46 to 306.7 mg m^{-2} d^{-1} (**Figure 3A**). The highest particle flux was in spring 2012 (April-May, from 306.7 to 180.2 mg m^{-2} d^{-1}). Additionally, three other events had relatively high particle fluxes: summer 2010 (June, 174.6 mg m^{-2} d^{-1}), 2011 (June,

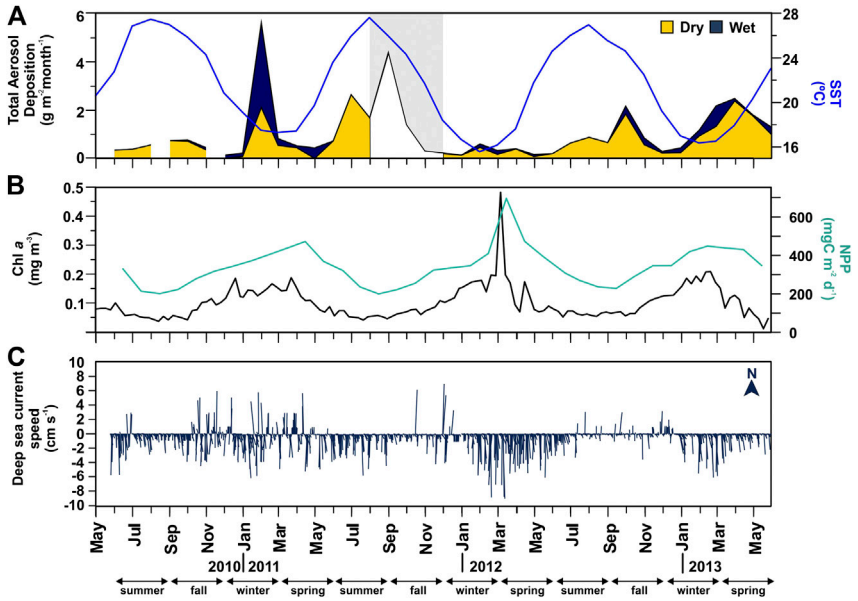

FIGURE 2 | Time-series of atmospheric and oceanographic parameters at the vicinities of the Ierapetra Basin station from June 2010 to June 2013. **(A)** monthly total aerosol [dry (yellow area) + wet (blue area)] deposition (in g m^{-2} $month^{-1}$) at the Finokalia station*, and monthly Sea Surface Temperature (SST, in °C, blue line); **(B)** 8-days surface Chlorophyll *a* concentration (Chl *a*, in mg m^{-3}), and monthly net primary production (NPP, in mg C m^{-2} d^{-1}, green line); and **C)** daily mean deep-sea current speed (in cm s^{-1}) and direction (º) at 4,287 m depth in the Ierapetra Basin (* gray area from September to November 2011 indicates values are available only for total atmospheric deposition, no distinction is made between dry and wet).

105.7 mg m^{-2} d^{-1}) and 2012 (June-July, from 123.2 to 104.5 mg m^{-2} d^{-1}).

During the three-year sampling period POC, opal, $CaCO_3$ and lithogenic fluxes were significantly and positively correlated with TMF (**Figure 4**). Lithogenic matter was the primary flux component, ranging from 0.04 to 156.1 mg m^{-2} day^{-1} and accounting for 86.6 ± 1.2% of TMF on average. Biogenic minerals were the next most abundant, with $CaCO_3$ (0.34–69.5 mg m^{-2} d^{-1}) and opal (0.03–58.7 mg m^{-2} d^{-1}) accounting for 28.6 ± 16.6% and 3.9 ± 4.1%, respectively, of TMF on average. OM contributed from 0.15 to 24.5 mg m^{-2} d^{-1}, accounting for 6.0 ± 3.2% of TMF on average.

POC fluxes ranged from 0.08 to 12.24 mg m^{-2} d^{-1}, and during 64% of the three-years studied the POC flux was <0.60 mg m^{-2} d^{-1} (**Figure 3C**). POC fluxes significantly correlated with the different mineral fractions: lithogenic (r = 0.83, slope = 0.051), $CaCO_3$ (r = 0.93, slope = 0.14) and opal fluxes (r = 0.97, slope = 0.21) (**Figures 4A** and **5**). Correlation of POC *vs* POC percentages was not significant. The highest percentages of POC were observed during the lowest flux periods in fall (5.83 ± 0.80%) and winter 2011 (5.00 ± 0.40%) (**Figure 3B**). POC percentages significantly and negatively correlated with lithogenic percentages, and positively with $CaCO_3$ and opal percentages (**Figure 4A**, **Supplementary Figure S1**).

The opal/$CaCO_3$ mole ratio ranged from 0.01 to 1.60, with an average value of 0.34 ± 0.36, and the POC/$CaCO_3$ mole ratio from 0.38 to 3.58, with an average of 1.06 ± 0.74 (**Table 1**). These two ratios visibly exhibit similar trends, which are positively correlated (r = 0.51, p = 0.004), with the highest opal/$CaCO_3$ and POC/$CaCO_3$ ratios during summer-fall 2011 and spring 2012. The POC/opal ratio ranged from 1.04 to 83.9, with an average of 7.23 ± 15.3, and exhibited exponential negative correlation with opal/$CaCO_3$ (r = 0.73, p < 0.0001).

Bulk Geochemical and Molecular Proxies

TN/POC and $\delta^{13}C$

Total nitrogen (TN) *vs* POC content presents a significant positive correlation (**Figure 4**). The TN/POC molar ratio of the sinking particles ranged from 0.11 to 0.25, with an average of 0.15 ± 0.04 (**Figure 3D**). This ratio was highest during fall 2010 and lowest during fall 2012. The $\delta^{13}C$ values of the sinking POC ranged from −26.53 to −21.33‰, with an average of −24.24 ± 0.96‰ (**Figure 3D**). The heaviest $\delta^{13}C$ was observed during the high-flux period of spring 2012 and the lightest during the relatively low-flux period in winter 2010.

Lipid Biomarkers

The major marine C_{27}-C_{30} sterols considered in this study are cholesterol ($C_{27}\Delta^5$), brassicasterol ($C_{28}\Delta^{5,22E}$), β-sitosterol ($C_{29}\Delta^5$) and dinosterol ($4\alpha C_{30}\Delta^{22E}$). They show total fluxes ranging from 0.15 to 15.8 µg m^{-2} d^{-1}, and concentrations ranging between 4.53 and 1,100 µg g^{-1} (normalized to POC from 0.31 to 31.9 µg mg OC^{-1}) (**Figure 6**, **Table 2**). Cholesterol was the most abundant C_{27}–C_{30} sterol, with fluxes ranging from 0.09 to 14.7 µg m^{-2} d^{-1} at 4,285 m depth, with the highest recorded during spring 2013, spring 2012 and early summer 2011, and the lowest during fall-winter (**Figure 6A**). Cholesterol concentrations ranged between 1.97 and 868 µg g^{-1} (from 0.14 to 29.6 µg mg OC^{-1}). Brassicasterol, dinosterol and β-sitosterol followed similar flux and concentration trends as

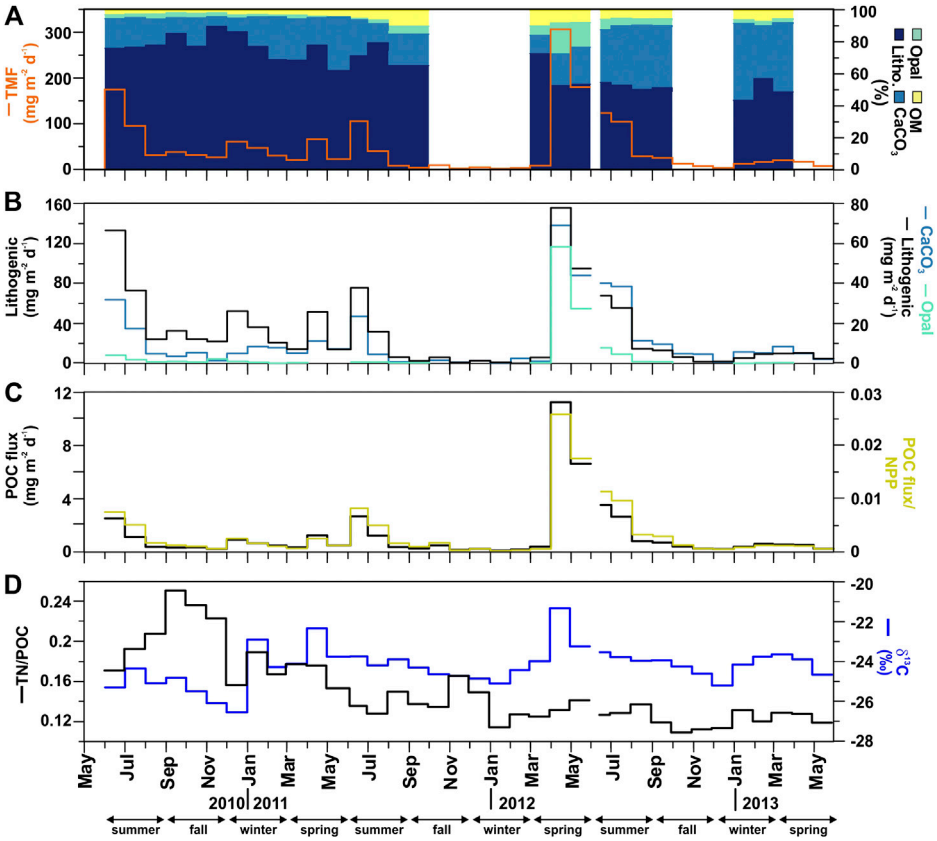

FIGURE 3 | Time-series at the Ierapetra Basin station from May 2010 to June 2013 of **(A)** Total Mass Flux (TMF, in mg m^{-2} d^{-1}), and cumulative percentages* of organic matter (OM), opal, carbonates ($CaCO_3$) and lithogenic; **(B)** Fluxes of lithogenic, opal and $CaCO_3$; **(C)** Particulate organic carbon (POC) flux, and export efficiency ratio (POC flux/NPP); **(D)** TN/POC molar ratio and $\delta^{13}C$ stable isotope (*Gaps of cumulative percentages of flux components correspond to periods where there are no opal data available).

cholesterol, positively correlated (**Figure 4**), but with up to an order of magnitude lower, except during spring of 2012 (**Figure 6B**, **Table 2**). The fluxes of long-chain C_{30} *n*-alkan-1,15-diols and the corresponding C_{30} keto-ols together ranged from 0.01 to 0.70 μg m^{-2} d^{-1}, with the highest values during spring 2012, fall 2011 and winter 2010 (**Figure 6E**). Concentrations ranged from 0.18 to 43.3 μg g^{-1} (from 0.02 to 0.42 μg mg OC^{-1}). Long-chain alkenones, had total fluxes from 0.02 to 1.81 μg m^{-2} d^{-1}, and concentrations from 0.53 to 25.6 μg g^{-1} (from 0.02 to 0.87 μg mg OC^{-1}) (**Figure 6F**). Highest fluxes and concentrations are observed during spring. The fluxes of ∑Phyto, marine phytoplankton-derived lipids, ranged from 0.02 to 5.52 μg m^{-2} d^{-1} and POC-normalized concentrations ranged from 1.07 to 8.99 μg mg OC^{-1} (**Table 2**).

Total aliphatic hydrocarbons (AH) fluxes ranged from 0.44 to 40.6 μg m^{-2} d^{-1}, averaging 3.91 μg m^{-2} d^{-1}. Highest AH fluxes are observed during spring 2012, and in early summers 2010, 2011 and 2012. Total AH concentrations ranged from 23.2 to 492 μg g^{-1} (average 124 μg g^{-1}). POC normalized AH concentrations are 1.07–8.99 μg mg OC^{-1}, with the highest concentrations during fall (**Table 2**). The molecular profile of sinking particle-associated AH is dominated in all cases by a UCM and a series of resolved compounds. UCM, appearing as a unimodal hump centered around *n*-C_{30}, was the major component of sinking particle-associated AH, accounting for up to 91% of their total sum (67% on average). UCM fluxes ranged from 0.29 to 28.7 μg m^{-2} day^{-1}, averaging 3.04 μg m^{-2} day^{-1} (**Figure 7A**). The highest UCM flux was recorded in May 2012, a month after the maximum TMF. UCM concentrations ranged from 15.6 to 372 μg g^{-1}, and from 0.82 to 7.93 μg mg OC^{-1}. *n*-alkanes were the main AH resolved compounds accounting for up to 72% (average 31%) of their total sum and for up to 18% of total AH (average 3.1%). Total *n*-alkanes (∑*n*-$C_{24–33}$) fluxes were 0.04–4.12 μg m^{-2} d^{-1}, and concentrations 0.74–8.45 μg g^{-1} and 0.11–1.31 μg mg OC^{-1}. During the study period, their molecular profile is dominated by long-chain homologues (*n*-C_{20} to *n*-C_{35}) with a CPI_{NA} value from 1.10 to 4.73. Highest CPI_{NA} were observed for summer 2011, and lowest for spring 2012 coupled with the highest UCM flux (**Figures 7A,D**). The flux of the most abundant high molecular weight plant wax *n*-alkanes corrected for the contribution of oil-derived long chain odd-numbered homologues (∑TerNA) ranged from 0.01 to 0.72 μg m^{-2} d^{-1}, and concentrations ranged from 0.74 to 8.45 μg g^{-1} (from 0.06 to 0.27 μg mg OC^{-1}) (**Figure 7B**).

The aliphatic alcohol fraction in the sinking particle samples is dominated in all cases by *n*-C_{24} to *n*-C_{30} alkanols with a maximum at *n*-C_{26}. The plant wax *n*-alkanols (∑TerN-OH) fluxes ranged from 0.03 to 1.65 μg m^{-2} d^{-1}, with the highest

TABLE 1 | Total mass fluxes (TMF) and bulk composition of sinking particles collected at 4,285 m in the Ierapetra Basin (n.d.: no data).

opening day	Sampling days	Season	ID—Bottle	TMF (mg m^{-2} d^{-1})	POC (%)	TN (%)	$\delta^{13}C$ (‰)	Opal (%)	$CaCO_3$ (%)	Lithogenic (%)	$POC/CaCO_3$	POC/opal	$Opal/CaCO_3$
01-Jun-10	30	Summer	RED I-1	174.6	1.42	0.28	−25.29	2.42	18.4	76.3	0.64	2.94	0.22
01-Jul-10	31	Summer	RED I-2	95.1	1.15	0.26	−24.35	2.19	18.5	77.0	0.52	2.63	0.20
01-Aug-10	31	Summer	RED I-3	31.0	1.13	0.27	−25.08	3.21	16.3	78.3	0.58	1.76	0.33
01-Sep-10	30	Fall	RED I-4	38.2	0.75	0.22	−24.81	3.05	9.87	85.6	0.63	1.23	0.51
01-Oct-10	31	Fall	RED I-5	31.3	0.97	0.27	−25.48	2.72	17.7	77.7	0.46	1.78	0.26
01-Nov-10	30	Fall	RED I-6	26.3	0.77	0.20	−26.08	2.45	6.06	83.4	1.06	1.58	0.67
01-Dec-10	31	Winter	RED I-7	60.4	1.46	0.26	−26.53	1.95	8.53	86.6	1.42	3.74	0.38
01-Jan-11	31	Winter	RED I-8	47.0	1.31	0.29	−22.91	1.49	18.4	77.5	0.59	4.40	0.13
01-Feb-11	28	Winter	RED I-9	30.1	1.48	0.29	−24.28	1.08	26.7	69.3	0.46	6.84	0.07
01-Mar-11	31	Spring	RED I-10	20.6	1.50	0.31	−24.10	2.43	25.7	68.9	0.49	3.09	0.16
01-Apr-11	30	Spring	RED I-11	66.1	1.83	0.37	−22.35	0.79	17.3	78.3	0.88	11.59	0.08
01-May-11	31	Spring	RED I-12	22.3	2.01	0.36	−23.76	0.12	33.4	62.4	0.50	83.94	0.01
05-Jun-11	26	Summer	RED II-1	105.7	2.50	0.39	−23.74	0.84	22.5	71.7	0.93	14.90	0.06
01-Jul-11	31	Summer	RED II-2	39.8	2.99	0.44	−24.19	2.31	11.9	79.8	2.09	6.49	0.32
01-Aug-11	31	Summer	RED II-3	8.11	4.09	0.71	−23.89	4.31	12.4	75.1	2.75	4.75	0.58
01-Sep-11	30	Fall	RED II-4	3.80	6.03	0.96	−24.30	n.d.	24.3	63.6	2.07	n.d.	n.d.
01-Oct-11	31	Fall	RED II-5	9.10	4.95	0.77	−24.64	5.02	19.5	65.6	2.11	4.94	0.43
01-Nov-11	30	Fall	RED II-6	1.74	6.51	1.25	−24.71	n.d.	45.7	41.2	1.19	n.d.	n.d.
01-Dec-11	31	Winter	RED II-7	4.49	4.54	0.79	−24.85	n.d.	33.0	57.9	1.15	n.d.	n.d.
01-Jan-12	31	Winter	RED II-8	1.46	5.24	0.69	−25.09	n.d.	23.0	66.5	1.90	n.d.	n.d.
01-Feb-12	29	Winter	RED II-9	3.02	5.23	0.77	−24.42	n.d.	84.6	4.90	0.51	n.d.	n.d.
01-Mar-12	31	Spring	RED II-10	8.34	4.91	0.71	−23.98	5.78	11.4	73.0	3.58	4.25	0.84
01-Apr-12	30	Spring	RED II-11	306.7	3.99	0.61	−21.33	19.1	19.9	53.0	1.67	1.04	1.60
01-May-12	31	Spring	RED II-12	180.2	3.85	0.63	−23.24	15.3	23.1	53.9	1.39	1.26	1.11
15-Jun-12	16	Summer	RED III-1	123.2	2.83	0.42	−23.53	6.47	32.8	55.1	0.72	2.19	0.33
01-Jul-12	31	Summer	RED III-2	104.5	2.50	0.37	−23.78	4.64	37.1	53.3	0.56	2.69	0.21
01-Aug-12	31	Summer	RED III-3	28.9	2.69	0.43	−23.97	3.88	40.2	50.5	0.56	3.47	0.16
01-Sep-12	30	Fall	RED III-4	25.3	2.68	0.37	−23.94	4.15	38.8	51.7	0.57	3.22	0.18
01-Oct-12	31	Fall	RED III-5	12.5	3.04	0.38	−24.25	4.18	40.3	49.4	0.63	3.64	0.17
01-Nov-12	30	Fall	RED III-6	7.13	3.12	0.40	−24.60	n.d.	68.3	25.5	0.38	n.d.	n.d.
01-Dec-12	31	Winter	RED III-7	3.22	5.82	0.76	−25.20	n.d.	27.6	60.8	1.76	n.d.	n.d.
01-Jan-13	31	Winter	RED III-8	12.4	2.92	0.44	−24.16	2.32	48.0	43.8	0.51	6.30	0.08
01-Feb-13	28	Winter	RED III-9	16.4	3.47	0.48	−23.76	2.68	33.0	57.4	0.88	6.47	0.14
01-Mar-13	31	Spring	RED III-10	20.0	2.63	0.39	−23.64	2.53	43.1	49.1	0.51	5.20	0.10
01-Apr-13	30	Spring	RED III-11	16.9	2.94	0.43	−23.89	2.36	30.3	61.5	0.81	6.23	0.13
01-May-13	31	Spring	RED III-12	7.35	2.89	0.40	−24.66	n.d.	30.5	63.7	0.79	n.d.	n.d.

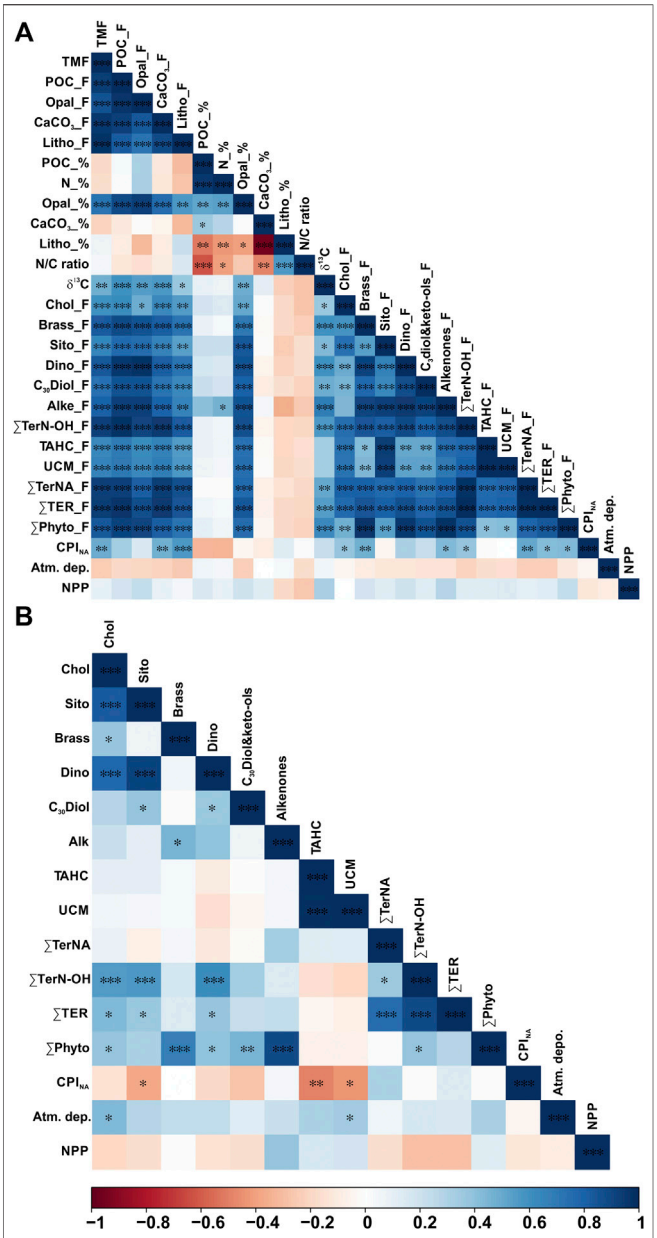

FIGURE 4 | Pearson correlation heatmap matrix with significance level expressed by asterisks (***p-value ≤ 0.001, **p-value ≤ 0.05, *p-value ≤ 0.1) of **A)** fluxes (F) and percentages (%) of bulk parameters, fluxes of lipid biomarkers, CPI_{NA}, total atmospheric deposition, and net primary production, and **(B)** POC-normalized concentrations of lipid biomarkers and CPI_{NA}, total atmospheric deposition, and net primary production. Positive correlations are displayed in blue and negative correlations in red color. Color intensity are proportional to the correlation coefficients.

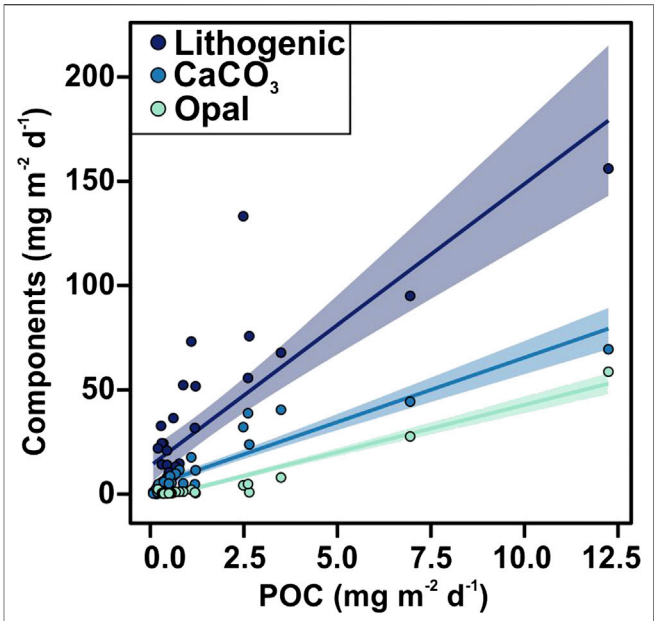

FIGURE 5 | Scatter plot of POC flux *vs.* lithogenic, $CaCO_3$ and opal material fluxes. The shaded areas represent prediction interval at the 95% confidence level.

fluxes during spring 2012, and early summer 2010, 2011 and 2012. Concentrations ranged from 1.22 to 22.5 μg g^{-1} and from 0.11 to 0.38 μg mg OC^{-1}, with the highest values during fall (**Figure 7C**). ∑TerN-OH and ∑Phyto POC-normalized concentrations showed a positive correlation (**Figure 4B**)

Land-derived lipid fluxes (∑Ter) ranged from 0.04 to 2.37 μg m^{-2} d^{-1}, with POC-normalized concentrations from 0.18 to 0.52 μg mg OC^{-1}. ∑Ter fluxes were positively correlated with ∑Phyto fluxes (**Figure 4**), with highest values during spring 2012 and summers 2010 and 2012 (**Figure 8**). Highest ∑Ter POC-normalized concentrations were during fall periods. POC-normalized concentrations of ∑Ter *vs.* ∑Phyto had a very weak positive correlation when considering all sinking particles (**Figure 8**). However, for each season individually, POC-normalized concentrations of ∑Ter *vs.* ∑Phyto of summer sinking particles showed a strong positive correlation (**Figure 8**, **Supplementary Figure S2**).

Multivariate Analysis

PCA was conducted to assess the compositional and temporal evolution of particle fluxes during the studied period. The first two principal components are responsible for 68.8% of the variance (**Figure 9A**). Factor 1 (PC1) explains 57.1% of the total variance and is characterized by positive loadings, above 0.7, for all bulk parameters, brassicasterol, dinosterol and ∑TerNA lipid fluxes, $\delta^{13}C$ and CPI_{NA}, and negative loadings, below −0.15, for SST and atmospheric deposition. PC1 separates samples according to particle fluxes, with the highest factor scores for the extreme episodic event on spring 2012, and summer months (**Figure 9B**). Thus, PC1 reflects the high particle flux periods and the impact of episodic events on the deep particle flux in the EMS. Factor 2 (PC2) explains another 11.7% of the variance and has positive loadings, above 0.7, for UCM, β-sitosterol, ∑TerN-OH fluxes, and negative loadings, below -0.15, for TN/POC ratio and CPI_{NA}. Therefore, PC2 separates samples by relative contribution of land-derived POC sources. Spring and summer samples showed the highest PC2 factor scores, and fall had the lowest. Factor 3 (PC3) explains 7.9% of the total variance

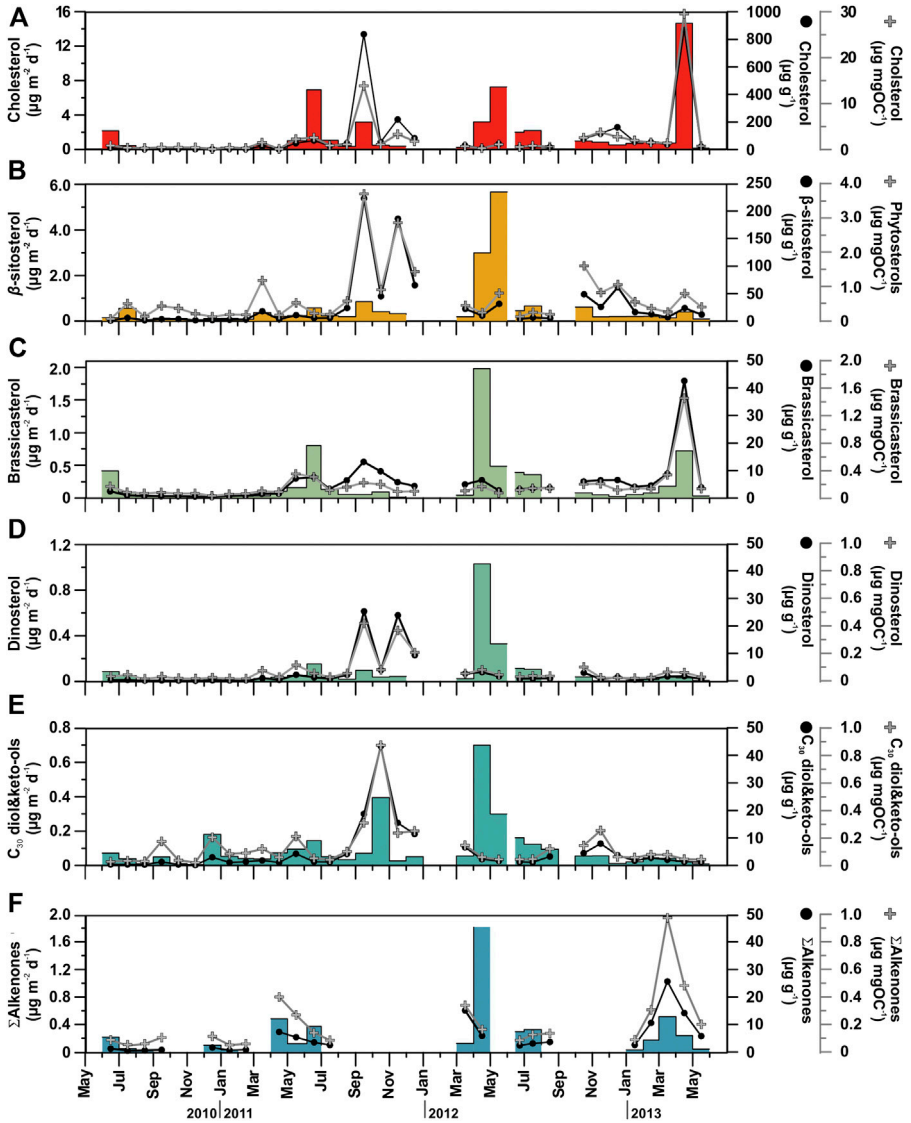

FIGURE 6 | Temporal distribution patterns (fluxes and concentrations) of major phytoplankton- and zooplankton-derived POC compounds (marine origin) in sinking particulate matter collected at 4,285 m in the Ierapetra Basin during the studied period (see section "**Oceanographic and Atmospheric Settings**". for further details).

and is characterized by positive loadings, above 0.5, for NPP, $\delta^{13}C$, and negative loadings, below -0.15, for SST, TN/POC ratio and CPI_{NA}. Highest PC3 factor scores were observed for spring samples. Therefore, PC3 separates samples by the relative contribution of phytoplankton-derived POC.

DISCUSSION

Efficiency of the Biological Pump in the Deep Ierapetra Basin

The mean annual TMF measured in the deep Ierapetra Basin (**Figure 3A**) is fairly comparable with those reported in previous studies that investigated particle fluxes in the bathypelagic EMS (e.g., Kerhervé et al., 1999; Stavrakakis et al., 2000; Patara et al., 2009; Karageorgis et al., 2018; Theodosi et al., 2019). For comparison, in the western Mediterranean Sea, TMF above 500 mg m^{-2} d^{-1} has been reported in the Alboran Sea (e.g., Fabres et al., 2002; Sanchez-Vidal et al., 2005) and submarine canyons of the NW Mediterranean Sea (e.g., Zúñiga et al., 2009; Stabholz et al., 2013).

POC fluxes recorded in this study are also of the same order of magnitude as those reported in previous studies that investigate POC fluxes in the deep EMS. The low POC fluxes during winter and spring are in line with the POC fluxes measured at 2,700 m in the Ierapetra Basin by Koppelmann et al. (2004) during winter/early spring 1999 (0.25–0.57 mg m^{-2} d^{-1}, from January to March) and late spring 1999 (1.16 mg m^{-2} d^{-1} during April). Karageorgis

TABLE 2 | POC-normalized concentrations of selected lipid biomarkers (n.d.: no data).

Opening day	ID - Bottle	Cholesterol $C_{27}\Delta^{5}$ (µg mg OC^{-1})	Brassicasterol $C_{28}\Delta^{5,22E}$ (µg mg OC^{-1})	Dinosterol $4\alpha C_{30}\Delta^{22E}$ (µg mg OC^{-1})	β-sitosterol $C_{29}\Delta^{5}$ (µg mg OC^{-1})	C_{30} diols& keto-ols[a] (µg mg OC^{-1})	Alkenone[b] (µg mg OC^{-1})	Total AH (µg mg OC^{-1})	UCM (µg mg OC^{-1})	∑TerNA (µg mg OC^{-1})	∑TerN-OH (µg mg OC^{-1})
01-Jun-10	RED I-1	0.87	0.17	0.03	0.06	0.03	0.09	1.95	1.42	0.15	0.18
01-Jul-10	RED I-2	0.41	0.08	0.05	0.51	0.04	0.05	2.02	1.36	0.09	0.20
01-Aug-10	RED I-3	0.32	0.06	0.02	0.13	0.03	0.06	2.85	2.13	0.09	0.13
01-Sep-10	RED I-4	0.48	0.08	0.03	0.44	0.18	0.10	4.71	3.91	0.10	0.16
01-Oct-10	RED I-5	0.48	0.06	0.02	0.37	0.04	n.d.	4.27	3.31	0.27	0.19
01-Nov-10	RED I-6	0.45	0.06	0.02	0.21	0.02	n.d.	5.45	4.18	0.26	0.26
01-Dec-10	RED I-7	0.14	0.03	0.03	0.12	0.21	0.11	5.65	5.10	0.06	0.12
01-Jan-11	RED I-8	0.42	0.05	0.02	0.19	0.09	0.05	2.72	2.15	0.08	0.11
01-Feb-11	RED I-9	0.32	0.06	0.02	0.18	0.09	0.06	8.71	7.93	0.09	0.11
01-Mar-11	RED I-10	1.51	0.10	0.08	1.18	0.12	n.d.	2.49	1.91	0.08	0.17
01-Apr-11	RED I-11	0.14	0.08	0.03	0.17	0.06	0.40	1.53	1.16	0.07	0.11
01-May-11	RED I-12	2.28	0.35	0.12	0.53	0.21	0.27	2.05	1.54	0.13	0.38
05-Jun-11	RED II-1	2.62	0.30	0.06	0.22	0.05	0.14	1.88	1.52	0.17	0.24
01-Jul-11	RED II-2	0.90	0.11	0.03	0.19	0.04	0.09	1.71	1.32	0.14	0.22
01-Aug-11	RED II-3	1.11	0.16	0.06	0.58	0.10	n.d.	2.48	1.74	0.08	0.25
01-Sep-11	RED II-4	13.9	0.22	0.42	3.72	0.31	n.d.	4.24	3.12	0.14	0.37
01-Oct-11	RED II-5	1.11	0.20	0.08	0.91	0.87	n.d.	2.87	1.96	0.15	0.25
01-Nov-11	RED II-6	3.36	0.09	0.37	2.87	0.24	n.d.	4.88	3.39	0.08	0.28
01-Dec-11	RED II-7	1.82	0.09	0.21	1.44	0.25	n.d.	2.14	1.44	0.07	0.25
01-Jan-12	RED II-8	n.d.	n.d.	n.d.	n.d.	n.d.	n.d.	n.d.	n.d.	n.d.	n.d.
01-Feb-12	RED II-9	n.d.	n.d.	n.d.	n.d.	n.d.	n.d.	n.d.	n.d.	n.d.	n.d.
01-Mar-12	RED II-10	0.61	0.10	0.06	0.46	0.13	0.31	4.88	3.92	0.11	0.22
01-Apr-12	RED II-11	0.26	0.16	0.08	0.24	0.06	0.15	1.07	0.82	0.06	0.14
01-May-12	RED II-12	1.05	0.07	0.05	0.82	0.04	n.d.	5.85	4.13	0.10	0.19
15-Jun-12	RED III-1	0.57	0.11	0.03	0.13	0.05	0.08	2.85	2.43	0.09	0.18
01-Jul-12	RED III-2	0.84	0.14	0.04	0.25	0.05	0.13	2.38	1.96	0.12	0.22
01-Aug-12	RED III-3	0.63	0.13	0.04	0.19	0.12	0.14	5.06	4.48	0.17	0.27
01-Sep-12	RED III-4	n.d.	n.d.	n.d.	n.d.	n.d.	n.d.	n.d.	n.d.	n.d.	n.d.
01-Oct-12	RED III-5	2.58	0.20	0.10	1.61	0.15	n.d.	4.84	4.07	0.17	0.33
01-Nov-12	RED III-6	3.76	0.21	0.03	0.83	0.25	n.d.	8.99	7.55	0.13	0.16
01-Dec-12	RED III-7	2.78	0.11	0.03	1.06	0.06	n.d.	8.45	6.38	0.12	0.16
01-Jan-13	RED III-8	1.97	0.14	0.02	0.56	0.06	0.09	4.47	3.70	0.11	0.16
01-Feb-13	RED III-9	1.53	0.13	0.03	0.37	0.08	0.31	4.66	3.80	0.17	0.20
01-Mar-13	RED III-10	1.42	0.33	0.07	0.26	0.08	0.97	4.31	3.58	0.17	0.19
01-Apr-13	RED III-11	29.6	1.45	0.06	0.81	0.05	0.48	5.26	4.33	0.11	0.20
01-May-13	RED III-12	0.76	0.13	0.03	0.41	0.04	0.20	8.69	7.71	0.12	0.18

[a]*Sum of the concentrations of long-chain C_{30} n-alkan-1,15-diols and C_{30} keto-ols.*

[b]*Sum of the concentrations of $C_{37:3}M$, $C_{37:2}M$, $C_{36:2}FAME$, $C_{38:3}Et$, $C_{38:3}M$, $C_{38:2}Et$, $C_{38:2}M$.*

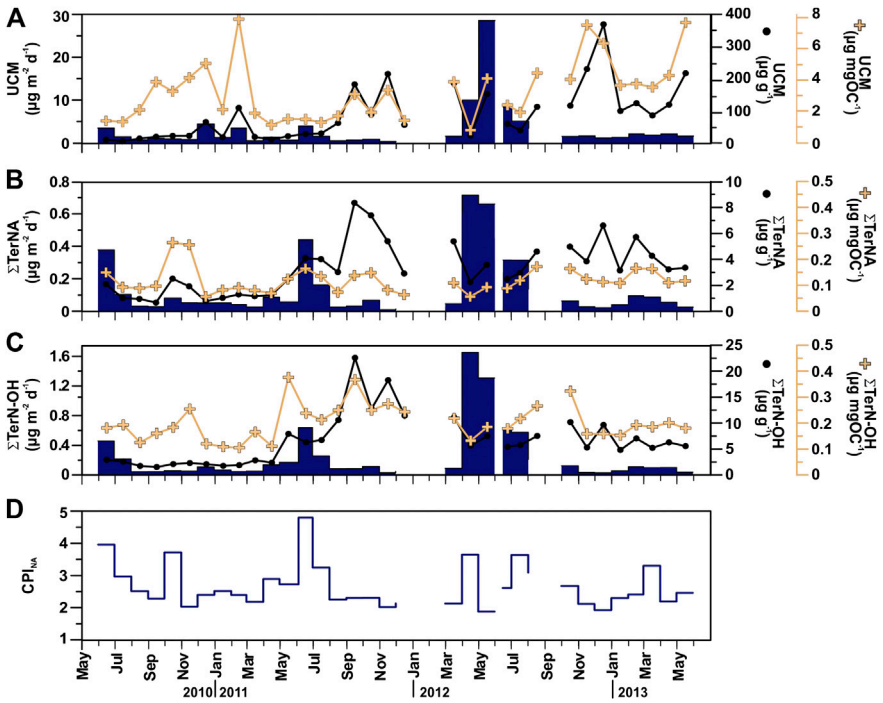

FIGURE 7 | Temporal distribution patterns (fluxes and concentrations) of major terrestrial and anthropogenic-derived POC compounds in sinking particulate matter collected at 4,285 m in the Ierapetra Basin during the studied period: **(A)** Unresolved Complex Mixture of aliphatic hydrocarbons (UCM), **(B)** long-chain *n*-alkanes (∑TerNa), and **(C)** long-chain *n*-alkanols (∑TerN-OH), and **(D)** Carbon Preference Index of long-chain *n*-alkanes (CPI_{NA}) (see section "**Source Indicators of Sinking Particulate Organic Carbon**" for further details).

et al. (2018) reported mean annual POC fluxes between 1.5 and 4.8 mg m^{-2} d^{-1} (May 2005 - June 2006) in the southern Cretan margin at depths from 1,215 to 3,538 m. Gogou et al. (2014) reported mean annual POC fluxes <6 mg m^{-2} d^{-1} (September 2007 to September 2008) in the southern Ionian Sea at 1,400 and 2,800 m water depth. Stavrakakis et al. (2013) reported mean annual POC fluxes between 0.01 and 12.3 mg m^{-2} d^{-1} (February 2006 to March 2010) in the SE Ionian Sea (NESTOR site) at depths from 1,200 to 4,300 m. Finally, Stavrakakis et al. (2000) reported POC fluxes <8.03 and <10.96 mg m^{-2} d^{-1} (November 1994 to November 1995) in the southern Cretan Sea at 200 m and 1,515 m water depth, respectively.

The low POC fluxes reported herein match the very low NPP observed in the Ierapetra Basin during the study period (~118 g C m^{-2} y^{-1}) and reported from other studies in the open waters of the Levantine Basin (97–113 g C m^{-2} y^{-1}) (Antoine et al., 1995; Napolitano et al., 2000; Bosc et al., 2004), which is lower than in the center of large oceanic gyres, such as the Sargasso Sea, where values around 150 g C m^{-2} y^{-1} have been measured (Steinberg et al., 2001; Lomas et al., 2013). For comparison, the primary productivity of coastal and upwelling zones, in some of the most productive areas of the ocean, typically exhibit values close to 250 g C m^{-2} y^{-1} (Longhurst et al., 1995). The fraction of primary production exported to the deep Ierapetra Basin averaged 0.35%, which is comparable to what has been observed in the EMS in the southern Ionian Sea at depths from 2,000 to 2,800 m (Stavrakakis et al., 2013; Gogou et al., 2014), but two-fold higher than what was reported at 4,300 m in the sourtheastern Ionian Sea (Stavrakakis et al., 2013).

Over the study period, the export efficiency was low during 66% (<0.02, twentieth percentile of data) of the time, and moderate during 30.6% of the time (between 0.2 and 0.02) (**Figure 3C**). This underscores the strong oligotrophic conditions of the study area. To further investigate the efficiency of the biological carbon pump we tested the correlation between the export efficiency (POC flux/NPP) and NPP (**Figure 11**). Herein we cannot conclude that in the EMS there is an inverse relationship between PP and export efficiency, as previously identified for the Southern Ocean (Maiti et al., 2013; Cavan et al., 2015; Le Moigne et al., 2016) and globally (Henson et al., 2019). We observed that, overall, there is no clear relationship between the export efficiency and NPP, except when observing seasonal trends (see discussion in section "**Seasonal Export Pulses to the Deep Eastern Mediterranean Sea**" below).

The POC content of sinking particles of the deep Ierapetra Basin (3.00 ± 1.60% POC) was 6-fold higher than the reported for deep-sea surface sediments in the study area (0.49 ± 0.09% POC). Thus, our data indicate that, on average, just about 16% of the POC that reaches the bathypelagic Ierapetra Basin gets settled and preserved to the seafloor sediments.

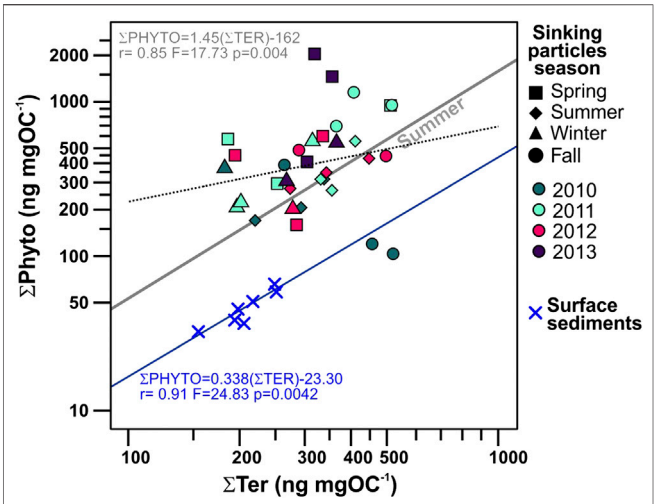

FIGURE 8 | Biplot of POC-normalized concentrations of phytoplankton-derived lipid biomarkers (ΣPhyto) *vs.* terrestrial (ΣTer) of sinking particles collected in the deep Ierapetra Basin from June 2010–June 2013, and surface sediments collected from January 2007 to June 2012 in the NW Levantine Basin (Pedrosa-Pàmies et al., 2015). Symbol shapes correspond to season of the sinking particles and colors correspond to sampling year. Regression lines for all (dashed black line, not significative) and summer period (gray line) sinking particles, as well as for surface sediments (blue line) are represented.

Drivers of Natural and Anthropogenic Particulate Organic Carbon Export

The positive correlation of POC fluxes with the different mineral fractions, especially with the biogenic minerals (**Figure 5**), observed throughout the study period suggests that the ballasting effect of the biogenic minerals is an important factor promoting the export of organic carbon to the deep EMS by increasing the density of settling particles, and/or providing POC protection against remineralization (Armstrong et al., 2002; Francois et al., 2002; Klaas and Archer, 2002). These correlations agree with the study from Klaas and Archer (2002) where they evaluated data from 52 sediment trap experiments worldwide. Low slope of opal *vs* POC flux suggest that in the EMS opal is more effective than carbonates at facilitating the POC flux.

Plankton and microbial community structure in the upper ocean also play a significant role in the export and transfer efficiency of carbon to the ocean interior (Herndl et al., 2008; Guidi et al., 2009; Henson et al., 2012). The main functional groups of phytoplankton contributing to export production through direct sedimentation are nitrogen fixers (e.g., diazotrophic cyanobacteria), silicifiers (e.g., diatoms), calcifiers (e.g., coccolithophores) and other marine plankton (e.g., dinoflagellates) (Agusti et al., 2015; Le Moigne et al., 2015; Turner, 2015; Basu et al., 2018). Generally, in the EMS there is a predominance of dinoflagellates and coccolithophores over diatoms (Malinverno et al., 2003; Ignatiades et al., 2009; Skampa et al., 2020 and references therein), except for the Rhodes gyre area under strong upwelling conditions where diatoms can be dominant (Siokou-Frangou et al., 1999). Therefore, the more stable POC/$CaCO_3$ ratio compared to the POC/opal ratio (**Table 1**) can be associated with the phytoplankton community dynamics and morphological and ecological differences between diatoms and coccolithophorids (De La Rocha and Passow, 2007). Moreover, the relatively high fluxes and POC-normalized concentrations of cholesterol ($C_{27}\Delta^5$) indicate that secondary production has a critical role exporting POC to the deep EMS.

Phytoplankton growth rate, and availability of CO_2, light and nutrients affect isotopic fractionation and thus the $\delta^{13}C$ of POC (Rau et al., 1992; Burkhardt et al., 1999). Winter and spring are the only two seasons when sinking particles reaching the deep Ierapetra Basin show a significant positive correlation (spring: $r = 0.98$, $p < 0.0001$; winter: $r = 0.90$, $p = 0.003$) with sinking POC flux and $\delta^{13}C$ values (**Figure 11**). Because primary production affects the CO_2 concentration near the producers, there is a positive correlation between $\delta^{13}C$ of the phytoplankton and primary production, and consequently, also with sinking POC fluxes (Deuser et al., 1968; Rau et al., 1992). This suggests that during summer and fall, either CO_2 was not depleted enough to cause detectable enrichment of ^{13}C, or $\delta^{13}C$ values were shaped by other processes than primary production. Factors contributing to the decline in $\delta^{13}C$ of POC values can be microbial activity (Lehmann et al., 2002) and inputs from the overlying surface waters of terrestrial or anthropogenic POC. $\delta^{13}C$ values in marine algae from low-to mid-latitude temperate seas vary from -18‰ to -22‰ (Goericke and Fry, 1994; Meyers, 1994; Harmelin-Vivien et al., 2008), whereas most terrestrial POC inputs from C3 plants are -25‰ to -28‰ (Hedges et al., 1997) and POC from crude oil and petroleum products has values between −28.5 and −28.9‰ (Rumolo et al., 2011, and references therein). Therefore, a significant incorporation of terrestrial and anthropogenic POC may be a cause of the more depleted $\delta^{13}C$ values in the summer and fall samples. The $\delta^{13}C$ of the sinking particles was significantly lighter (average isotopic change -1.9‰) than those of surface sediments (**Figure 11**). This isotopic change indicates isotopic discrimination during sinking processes and potential incorporation of allochthonous material from the deep EMS. The isotopic fractionation between sinking particles from the deep ocean and surface sediments has been previously reported (e.g., Fischer and Wefer, 1996; Nakanishi and Minagawa, 2003 and references therein), but this is the first study to document it for the EMS.

The deviation of the TN/POC ratios of the sinking particles from the classical Redfield ratio (Redfield et al., 1963), further indicates POC degradation processes of marine labile compounds during transport from surface waters to the deep Ierapetra Basin (**Figure 11A**). The overall higher TN/POC ratios from the sinking particles *vs* the seafloor sediments (**Figure 11**) further reflect the preferential degradation of labile nitrogen-enriched organic matter and the re-working of marine algal organic matter by zooplankton and benthic invertebrates during transport and deposition (Gogou and Stephanou, 2004; Lampadariou et al., 2009). Additionally, by comparing the lipid biomarker composition of sinking particles *vs* surface sediments, we can provide insight about the pre-depositional processing of the

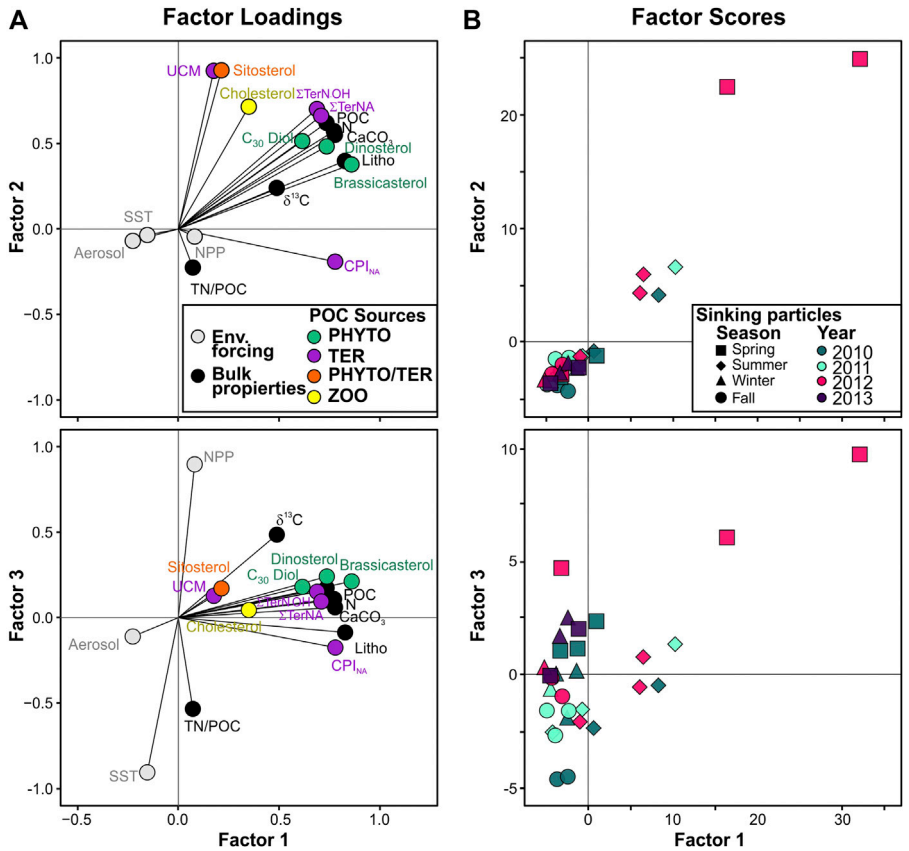

FIGURE 9 | PCA results. **(A)** Factor loadings for environmental forcing, bulk properties, and biomarkers of phytoplankton-derived POC (Phyto, green), zooplankton-derived POC (Zoo, yellow), and land-derived natural and anthropogenic POC (TER, purple) for the collected sinking particles. **(B)** Biplots of main factor scores for sinking particles identified by sampling year (colors) and season: fall (circle: September, October, November), spring (square: March, April, May), summer (diamond, June, July, August) and winter (triangle: December, January, February).

organic matter affecting the POC content and quality in the deep EMS before it gets buried. POC-normalized concentrations of phytoplankton- (∑Phyto) *vs* land-derived (∑Ter) lipid biomarkers of sinking particles compared with surface sediments (**Figure 8**) show that sinking particles are an order of magnitude more enriched in phytoplankton-derived POC, indicating the higher preservation efficiency of terrestrial *vs* marine POC (e.g., Hoefs et al., 2002; Burdige, 2007; Blair and Aller, 2012).

The weak negative correlation between molar TN/POC ratios and $\delta^{13}C$ values of the sinking particles (**Figures 4 and 11b**) indicates that the POC composition of the sinking particles was rather a mixture of marine (high TN/OC and $\delta^{13}C$) and terrestrial (low TN/OC and $\delta^{13}C$) particulate organic matter, but may also suggest significant contribution of other sources (e.g., anthropogenic POC). Indeed, the profile of AHs is indicative of the contribution of anthropogenic POC in the considered samples. Specifically, the CPI_{NA} values of long-chain *n*-alkanes ranging from 1.10 to 4.73 (**Figure 7d**), being, <2 in 61% of the cases, are indicative of a mixture of long straight-chain aliphatic compounds from both fossil (unburned fossil fuels) and land-derived (higher plant waxes) sources (Wang et al., 1999). Moreover, the presence of a UCM in all cases is indicative of anthropogenic POC deriving from degraded petroleum hydrocarbons and/or apolar products deriving from combustion processes (Wang et al., 1999). The entire EMS is a marine setting under intense anthropogenic pressure receiving substantial amounts of petroleum hydrocarbons through direct discharges from merchant shipping and oil transportation, mainly along shipping routes (Gogou et al., 2000; Parinos et al., 2013a; Parinos and Gogou, 2016; Hatzianestis et al., 2020). Furthermore, UCM hydrocarbons can also be derived from combustion processes, such as grass/wood/coal combustion and/or the incomplete combustion of fossil fuels, and are found in atmospheric aerosols collected from marine and urban areas of the EMS constituting a major source of combustion-related AHs through long-range atmospheric transport and subsequent dry/wet deposition (e.g., Tsapakis et al., 2006; Theodosi et al., 2013; Gogou et al., 1998 and references therein).

The strong positive correlation of UCM *vs.* POC fluxes (**Figure 4A**) is in agreement with the widely documented fact that the biogeochemical cycling of anthropogenic hydrocarbons

in marine systems is largely controlled by the biological pump and physico-chemical properties of individual compounds (Farrington and Takada, 2014, and references therein). Fossil hydrocarbons introduced into surface waters via the direct release of petroleum products by ships are more available to the dissolved phase, and are efficiently scavenged by organic rich particles (e.g., phytoplankton and fecal pellets), resulting in their sinking in open seas. Direct and indirect evidence of biodegradation has been shown as an important factor affecting their abundance during their downward transport in the water column. On the other hand, hydrocarbons derived from combustion sources, which are mainly introduced into surface EMS waters through long-range atmospheric transport and subsequent dry/wet deposition, are strongly associated to fine combustion particles that protect them from degradation during their transport through the water column. Sorption of combustion particles onto biogenic aggregates has been highlighted as the important mechanism regulating their cycling in marine systems (Deyme et al., 2011; Parinos et al., 2013b; Theodosi et al., 2013 and references therein)

Seasonal Export Pulses to the Deep Eastern Mediterranean Sea

Export during summer periods in the deep Ierapetra Basin was approximately four-fold greater than the export in wintertime, fall and springtime (except for the episodic event in spring 2012). In summer, the highest relative contribution of lithogenic to the TMF and relatively high POC fluxes coincided with the lowest NPP and high atmospheric dry deposition (**Figures 2** and **3**). It is well-documented that in the Levantine Basin the lowest Chl *a* and primary production levels and the highest transparency are found during the thermally stratified summer period (Gotsis-Skretas et al., 1999; Bosc, 2004; Ignatiades et al., 2009). Our results indicate that the export efficiency is relatively high during summer in the Levantine Basin (below **Figure 3C**). This rather high export efficiency in summertime has been previously reported in a wide range of open oceanic regions (Buesseler, 1998; Henson et al., 2012; Karl et al., 2012; Puigcorbé et al., 2015; Smith et al., 2018), and highlighted by biogeochemical models (Henson et al., 2015). The export efficiency can be highly variable depending on the degree of (de-)coupling between phytoplankton community structure (Buesseler, 1998; Francois et al., 2002), and upper ocean remineralization by zooplankton (Steinberg et al., 2002; Dagg et al., 2014; Cavan et al., 2015) and bacteria (Buchan et al., 2014; Belcher et al., 2016; Le Moigne et al., 2016; Henson et al., 2019). Sinking velocities in the EMS have been estimated to be 100–200 m d^{-1}, and are accelerated by pulses of primary production and grazing and by Saharan dust events that fertilize the upper ocean (Patara et al., 2009)

The fact that the relatively high POC fluxes in summer were enriched with land-derived natural AHs (higher plant waxes) as inferred from both ∑TerNA and ∑TerN-OH concentrations and elevated CPI_{NA} ratio values), anthropogenic AHs (UCM) (relatively high PC1 and PC2 scores), but also from phytoplankton- and zooplankton-derived lipids suggests that POC export to the deep EMS in summer is controlled by the interactions between the biological pump and different types of ballast minerals (dust/-induced POC export by fertilization and aggregation/adsorption processes) (Marañón et al., 2010; Bressac et al., 2014; van der Jagt et al., 2018).

Moreover, the relatively high fluxes of brassicasterol, dinosterol and C_{30} diols&keto-ols, and low POC-normalized concentrations of these phytoplankton-derived lipids coupled with high cholesterol fluxes and relatively high POC-normalized concentration of cholesterol (**Figure 6**), suggest that zooplankton has a significant role in the particle flux and POC degradation in summertime through grazing and repackaging in fecal pellets. This is consistent with previous studies that have reported relatively high export efficiencies during summer, when grazing is able to keep pace with NPP so that the POC flux via fecal pellets increases (Henson et al., 2015). Summertime nutrient limitation in the EMS leads to lower biological production and a plankton community structure dominated by small pico-autotrophic cells (<3 μm) (Psarra et al., 2000; Meador et al., 2010; Siokou-Frangou et al., 2010; Varkitzi et al., 2020). Raveh et al. (2015), revealed that autotrophic cyanobacteria such as *Synechococcus* and *Prochlorococcus* generally dominate the phytoplankton biomass during summer in the eastern Levantine Basin, and are also the main contributors to primary production. Small phytoplankton cells have a higher surface area-to-volume ratio, nutrient assimilation efficiency, photosynthetic activity, faster division rates and lower sinking rates than larger phytoplankton (Raven, 1998; Finkel et al., 2010). Therefore, picoautotroph-dominated communities during summer in the EMS may represent food webs with a high degree of aggregate repackaging with potential for accelerated sinking (Buesseler and Boyd, 2009; Bach et al., 2016).

The strong positive correlation of POC-normalized concentrations of ∑Ter *vs.* ∑Phyto of summer sinking particles (**Figure 8**), but also fluxes of UCM *vs.* ∑TerNA, ∑TerN-OH and ∑Phyto (**Figure 4**, **Supplementary Figure S2**), suggest that coupled with the plankton dynamics, the mineral ballast plays an important role in the export of natural and anthropogenic POC to the deep EMS during summer. For the EMS the periods of increased atmospheric dust are in spring and early summer, followed by autumn, and the dust sources are from the coasts of Africa, Arabian Peninsula and Red Sea (Moulin et al., 1998; Israelevich et al., 2012). Strict dry deposition is a highly effective mechanism of dust deposition in the Mediterranean Sea, and in summer it can contribute up to 93% to the total dust deposition due to the reduction or even absence of wet deposition (Kubilay et al., 2000). The highest summertime atmospheric deposition values were recorded in 2011. During this period, high aerosol dry deposition was recorded, associated with air masses from the south, carrying significant amounts of desert dust, and also air masses marked by local influence (**Supplementary Figure S3**).

In winter-spring (November to May) Chl *a* concentration increased (**Figure 2B**) but compared to summer, POC fluxes to the deep Ierapetra Basin were relatively low (**Figure 3B**), with exceptions, such as spring of 2012 (see discussion below in section "**Extreme Episodic Event in Spring 2012: Coupling of**

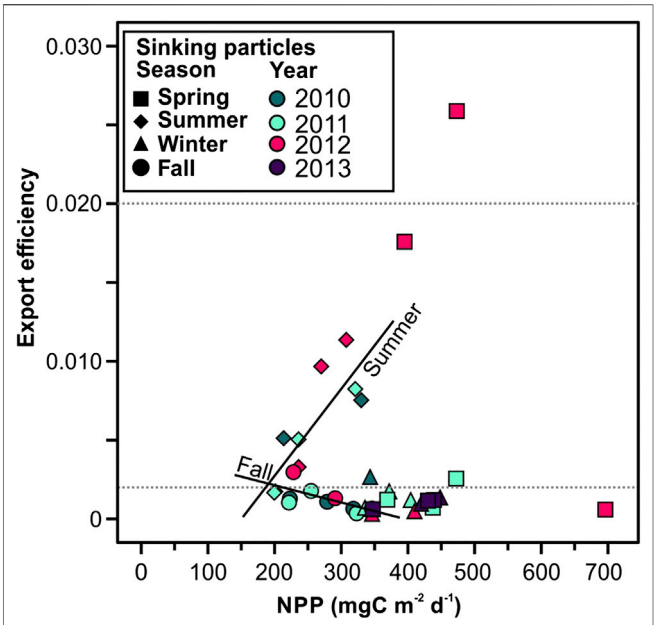

FIGURE 10 | Net primary productivity (NPP) plotted against export efficiency (POC flux/NPP). Horizontal dashed lines indicate threshold for export efficiency regimes: high export efficiency is defined as >0.2 (eightieth percentile of data), low export efficiency is <0.02 (twentieth percentile), and moderate export efficiency lies between. Significative regression lines are shown for summer (Export efficiency = 0.00006NPP–0.0082, $r = 0.824$, $p < 0.05$), and fall (Export efficiency = –0.00001NPP+0.0043, $r = 0.661$, $p = 0.053$).

Atmospheric Conditions Funneled Labile and Recalcitrant POC to the Deep EMS"). The low export efficiency can be explained by the tight coupling between primary producers and their grazers in the upper ocean layers (Henson et al., 2019 and references therein). The highest fluxes and POC-normalized concentrations of alkenones, and relatively high POC-normalized concentrations of brassicasterol, coupled with relatively enriched $\delta^{13}C$ values, in early spring sinking particles (March/April) (relatively high PC3 factor scores) (**Figure 9**), suggest that this tight coupling is broken intermittently during the onset of the spring bloom, allowing a small export pulse of labile phytoplankton-derived POC to the deep sea. Spring (excluding episodic event 2012) is the only season were we found positive trend of UCM *vs.* ∑Phyto fluxes ($r = 0.60$, $p = 0.15$), but also significant positive correlations of UCM fluxes and POC-normalized values *vs* atmospheric dry deposition ($r = 0.73$ $p = 0.06$, $r = 0.67$ $p = 0.10$, respectively). This suggests that long-range atmospheric transport of combustion emissions is the major source of these compounds, with subsequent sorption of the fine combustion particles onto biogenic aggregates likely regulating their sinking to the deep Ierapetra Basin. A clear coupling of this process is observed in spring of 2013 (March to May), which had relatively high ∑Phyto and UCM concentrations, and was a period with relatively high atmospheric deposition, with air masses arriving at Finokalia enriched in material from land, affected by both south and north continental areas surrounding the Mediterranean Sea (**Supplementary Figure S4**).

Fall and winter had the lowest particle and POC fluxes. These low fluxes could be explained by the microbial communities in the mesopelagic zone reducing sinking velocity of particles during this period and thus low export to the deep Ierapetra Basin (Sempéré et al., 2000; Herndl and Reinthaler, 2013). This hypothesis of POC reworking by microbial communities is supported by the very low POC-normalized concentrations of labile phytoplankton-derived lipids (i.e., brassicasterol and dinosterol), and cholesterol (lowest PC3 factor scores) (**Figure 9**). Fall is the only season where we observed an apparent relationship between NPP and export efficiency (**Figure 10**). This could imply that NPP become decoupled from the processes acting to remineralize POC in the upper ocean during fall periods.

Additionally, during fall period, it is particularly noteworthy to highlight September 2011, which had high total atmospheric deposition (**Figure 2A**). Air masses had significant continental and regional influence, coming from the northeast and east (sweeping the Balkans and Turkey), but also from the west (African continent) (**Supplementary Figure S5**). Therefore, during this period atmospheric deposition provided terrestrial material enriched in soil dust and vegetation, as imprinted in elevated land-derived terrestrial lipids (∑TerNA and ∑TerN-OH) POC-normalized concentrations and CPI_{NA} values (**Figure 7**). Interestingly, the highest POC-normalized concentrations of UCM (but also ∑TerNA, ∑TerN-OH and β-sitosterol) are recorded during late fall and winter periods. This could be attributed to the fact that fall/winter periods have the highest atmospheric wet deposition, especially in February 2011 (**Figure 2A**). During this month, air masses were significantly influenced by land, both coming from the Atlantic close-by the northwest Africa and reaching the EMS after having swept Central and Eastern Europe, and also directly coming from the African continent (**Supplementary Figure S6**). Atmospheric scavenging by rain drops of hydrocarbons emitted from anthropogenic (mainly air masses originating from the NW/N/NE sector) and terrestrial sources (from the SW/S sector), and subsequent efficient sorption of these hydrocarbons on organic-rich particles is likely the main mechanism driving their cycling during this period.

Extreme Episodic Event in Spring 2012: Coupling of Atmospheric Conditions Funneled Labile and Recalcitrant POC to the Deep EMS

In spring 2012, TMF and POC fluxes were one and two orders of magnitude, respectively, higher than in other spring periods over the study period (**Figure 3C**). As highlighted by Pedrosa-Pàmies et al. (2016), winter and spring of 2012 were characterized by exceptional atmospheric conditions. During winter 2011–12, particularly strong cold and dry northerly winds triggered intense convection not only in the EMS but also in the NW Mediterranean Sea (Durrieu de Madron et al., 2013; Palanques and Puig, 2018), and in the Adriatic Sea (Bensi et al., 2013; Janeković et al., 2014). The intense convection in winter 2012 caused an upwelling of relatively nutrient-rich cold water masses into the euphotic zone, triggering an exceptional phytoplankton

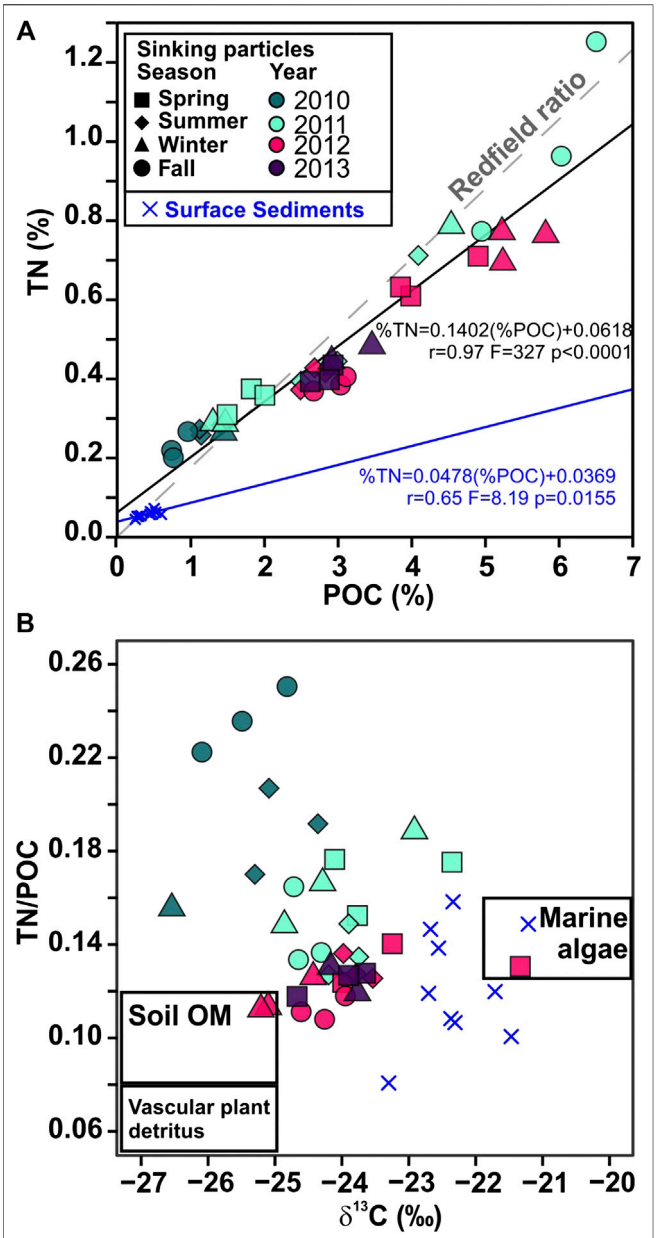

FIGURE 11 | (A) Plot of the weight percent content of nitrogen (TN) *vs.* particulate organic carbon (POC) in settling particles, and surface sediments samples from Pedrosa-Pàmies et al. (2015). The linear fit of the data is shown (solid line) along with the Redfield ratio N_{16}/C_{106} associated with the fresh marine phytoplankton (0.17 *wt/wt*, dashed line), **(B)** Plot of molar TN/OC ratios *vs.* $\delta^{13}C$, in the sediment trap and surface sediment samples. The compositional ranges of end members of organic matter sources (boxes) are derived from previously published studies (Meyers, 1994; Goñi and Hedges, 1995; Hedges et al., 1997; Harmelin-Vivien et al., 2008; Sanchez-Vidal et al., 2013). Symbol shapes correspond to season and colors correspond to sampling year.

bloom on March 2012 (**Figure 2B**). As emphasized by Pedrosa-Pàmies et al. (2016), the exceptional phytoplankton bloom was most probably stimulated by the arrival of Si and Fe from airborne Etna volcano ash during March-April 2012. Volcanic eruptions have the potential to cause regional or even global-scale nutrient (mainly Fe)-fertilization (Olgun et al., 2013; Browning et al., 2015; Weinbauer et al., 2017).

Mount Etna experienced high paroxysmal volcanic activity from January 2011 to April 2012 (Scollo et al., 2014; Giacomoni et al., 2018). In February 2012, the air masses that arrived at Finokalia station from the west had passed over south Italy/Sicily, thus collecting pollutants emitted from Etna (**Supplementary Figure S7**). Similarly, during March air masses remained of west sector and were influenced by volcanic activities in the Etna region together with marine emissions from the Mediterranean Sea, but also from land emissions over Africa (first part of the month) and Central Europe and long-range transport (second part of the month) (**Supplementary Figure S8**). Therefore, atmospheric deposition during this month integrates all potential sources surrounding the East Mediterranean, including Etna's emissions, except the East sector source (sources in the Middle-East).

In spring 2012 there was the highest export efficiency of the study period (**Figure 3C**), indicating that there was a decoupling between primary producers and the grazing population, allowing a strong episodic export pulse to reach the deep Ierapetra Basin (highest PC1, PC2 and PC3 factor scores) (**Figure 9**). The results of this study highlights that POC fluxes during this reported extreme episodic event were enriched in natural and anthropogenic, marine- and land-derived, lipid biomarkers (as inferred from UCM fluxes and CPI_{NA} ratio values ~1) (**Figure 7**). In April 2012, the POC exported during this event shows the highest $\delta^{13}C$ values (−21.33‰) over the study period, suggesting a high contribution of POC derived from marine relatively to land-derived natural sources (Goericke and Fry, 1994; Harmelin-Vivien et al., 2008). It is particularly noteworthy that surface sediment samples collected in the deep Ierapetra Basin (i.e., BF1MC22, Ier01 and Red 11) showed similar $\delta^{13}C$ and TN/POC ratio as sinking particles from the episodic event of spring 2012 (**Figure 11B**), suggesting that pulses of sinking particles during extreme episodic events can have a major role in modulating the seafloor POC composition in the deep Ierapetra Basin.

During the same month, the highest fluxes of brassicasterol of the study period and the highest opal fluxes, indicate the enhanced sedimentation of relatively fresh diatoms reaching bathypelagic depths. Although dinosterol, C_{30}diol and alkenones fluxes also had their maxima in April 2012, the high mole ratios of opal/$CaCO_3$ and POC/$CaCO_3$ in the sinking particles (**Table 2**) suggest that the upwelling event preferentially exported siliceous plankton relative to calcareous plankton (although the calcareous plankton benefitted too). This conclusion agrees with the phytoplankton community dynamics of the Rhodes' Gyre, where high abundances of large diatoms have been found under extreme meteorological conditions resulting in nutrient enrichment (Siokou-Frangou et al., 1999; Siokou-Frangou et al., 2010). In upwelling regions, the phytoplankton communities are often dominated by large diatoms (Malviya et al., 2016).

Supportive to the above, is that the settling particles collected during this period were embedded in a mucilaginous matrix with a high abundance of ash spherules and highly diverse, well-preserved, medium-sized (5–300 μm) long-chain- forming

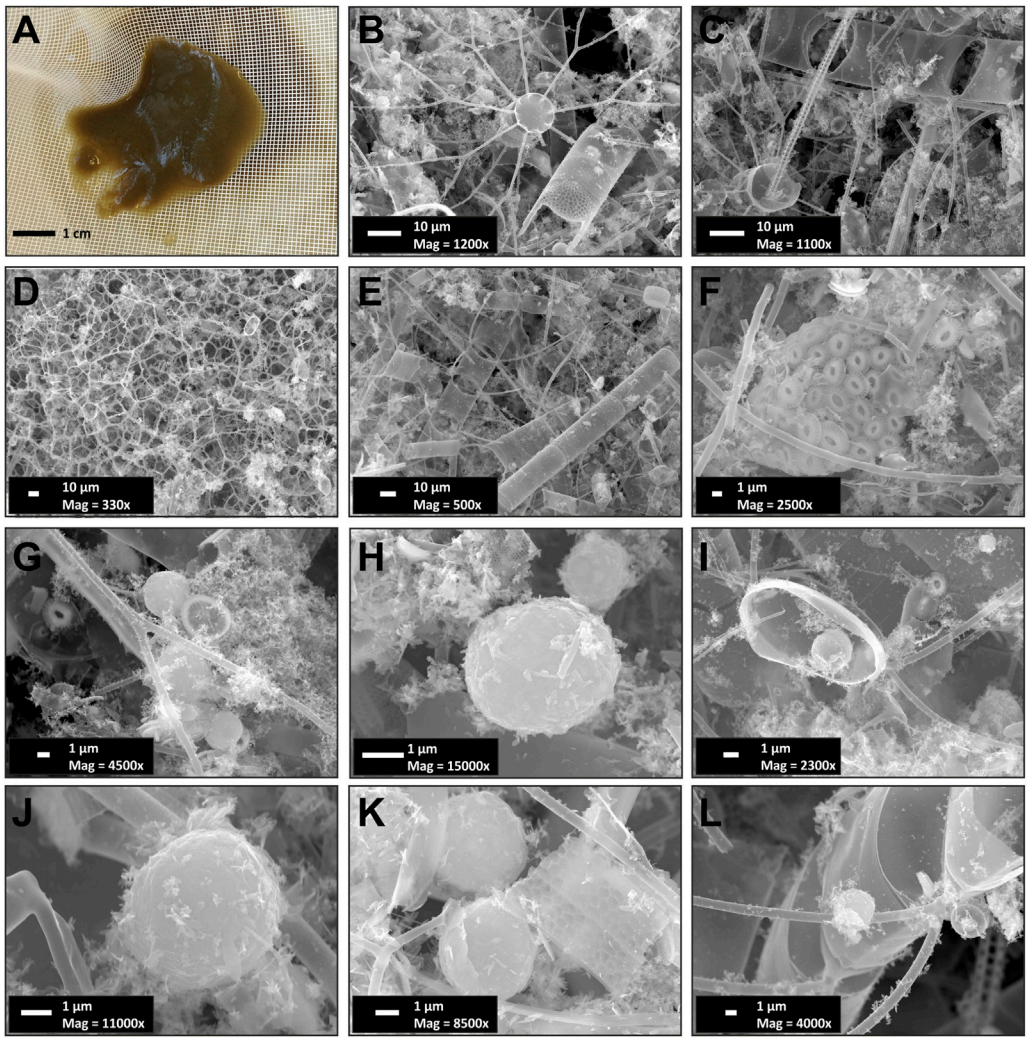

FIGURE 12 | Composite of **(A)** sample lab processing photo and **(B-I)** scanning electron microscopy (SEM) micrographs of sinking particles collected in April 2012 (REDII-11) in the deep Ierapetra Basin. Images reveal the abundant presence of well-preserved diatoms (**B–E**, e.g., *Chaetoceros* spp. and *Thalassioria* spp.), and coccolithophores **(F)** as well as ash microspherules **(G–L)**. Mag: Magnification (see more details in Pedrosa-Pàmies et al., 2016).

centric diatoms such as *Chaetoceros* spp., *Thalassiosira* spp., and *Rhizosolenia* spp (**Figure 12**). This mucilaginous matrix could be attributed to the production of transparent exopolymer particles (TEP) from diatom exudates rich in acidic polysaccharides (Gogou and Repeta, 2010). TEP increase the collision rates between particles, mostly in the form of large, rapidly sinking aggregates, playing an important role in carbon cycling in pelagic/oceanic ecosystems in general (Passow, 2002b and references therein) and the oligotrophic EMS in particular (Bar-Zeev et al., 2011; Parinos et al., 2017; Ortega-Retuerta et al., 2019). Diatoms have been reported to produce large amounts of TEP precursors or TEP directly via sloughing and lysis of senescent colonies under exponentially growing conditions (Passow, 2002a), such as in April of 2012, which are likely to have enhanced post-bloom flocculation and massive sinking of particulate matter in the study area. The ash particles, which typically have a density of twice that of seawater, could have also played an important role for rapid settling of biogenic particles (Passow and De La Rocha, 2006).

Furthermore, the exceptional diatom-dominated bloom fueled higher trophic levels, which further enhanced POC export. The covariation of the heterotrophic activity with the labile phytodetritus flux, producing a pulse of zooplankton-derived POC to the deep waters, is evidenced by the increase of cholesterol fluxes in April and May 2012 (3.20 and 7.23 $\mu g\ m^{-2}\ d^{-1}$, respectively) (**Figure 6A**). In the oligotrophic Sargasso Sea (N Atlantic), a similar ecosystem response has been observed as a result of the impact of mesoscale ocean features (fronts and eddies) (Conte et al., 1998, 2003) and extreme weather events (Pedrosa-Pàmies et al., 2019), locally enhancing vertical advection and stimulating production and sinking export of labile marine carbon to the deep ocean (e.g., increased cholesterol fluxes of 4.95 $\mu g\ m^{-2}\ d^{-1}$ at 3,200 m depth after a hurricane passage).

Sinking particles during this event were relatively depleted in land-derived natural POC and anthropogenic compounds due to dilution from biogenic material. Nevertheless, in April 2012, the highest fluxes of ∑TerNA and ∑TerN-OH, a decrease of CPI_{NA} and an increase in UCM fluxes (**Figure 7**) indicate that there was an efficient transfer of anthropogenic and higher plant wax-derived hydrocarbons to the deep Ierapetra Basin.

CONCLUSION

In the Ierapetra basin, particle flux data have been examined in combination with atmospheric and oceanographic parameters and main mass flux components (lithogenic, calcium carbonate, opal and organic matter), stable isotopes of POC ($\delta^{13}C$) and source-specific lipid biomarkers, aiming to improve the current understanding of the dynamics of particle fluxes and the impact of external forcing on the deep Eastern Mediterranean Sea. This study highlights that both seasonal and episodic pulses are crucial for POC export to the deep Ierapetra Basin, and likely most of the deep EMS. Overall, summer particle export to the deep EMS fuels more efficient carbon sequestration than during the other seasons. Our results also show that the combination of extreme weather events and aerosol deposition can trigger an influx of marine organic matter to the deep EMS. This influx is a critical factor determining food supply for deep ocean ecosystems, but also induces an increased influx of anthropogenic organic carbon to the deep EMS. Therefore, this study underscores the importance of accounting both seasonal and episodic pulses of POC to the deep sea when modeling the sequestration of natural and anthropogenic POC, and for a better understanding of the global carbon cycle. Finally, the comparison of biogeochemical parameters of the sinking particles flux data with previously reported surface sediments from the deep-sea in the study area revealed an isotopic discrimination, as also as a preferential degradation of labile organic matter during deposition and burial, along with higher preservation of land-derived POC in the underlying sediments. This line of research provides key knowledge to better understand the export, fate and preservation *vs.* degradation of marine and land-derived organic carbon and for modeling the organic carbon burial rates in the Mediterranean Sea.

DATA AVAILABILITY STATEMENT

The original contributions presented in the study are included in the article/**Supplementary Material**, further inquiries can be directed to the corresponding author.

AUTHOR CONTRIBUTIONS

RP-P performed the sample analyses and data processing and lead the interpretation of the results and wrote the manuscript. CP aided in interpreting the results and worked on the manuscript. RP-P and AS-V participated in the sample collection. AS-V and AC were involved in the design of the study, and supervised RP-P work during the early stage of the study. AG and CP supervised RP-P during the lipid biomarkers analyses at the Organic Chemistry Laboratory at HCMR. NL and MC were the REDECO's project co-ordinator and the lead of the University of Barcelona research team, respectively. DV contributed to the interpretation of the oceanographic settings of the study area. NM and MK contributed with Finokalia atmospheric observatory data and atmospheric data interpretation. All authors provided feedback on the manuscript.

FUNDING

This research was supported by the REDECO (CTM2008-04973-E/MAR) and PERSEUS (GA 287600) projects. We further acknowledge support by the projects PANACEA—'PANhellenic infrastructure for Atmospheric Composition and climatE chAnge' (MIS 5021516) and ENIRISST—'Intelligent Research Infrastructure for Shipping, Supply Chain, Transport and Logistics' (MIS 5027930), which are implemented under the Action "Reinforcement of the Research and Innovation Infrastructure," funded by the Operational Program "Competitiveness, Entrepreneurship and Innovation" (NSRF 2014-2020) and co-financed by Greece and EU; and by the Action "National Network on Climate Change and its Impacts - Climpact" which is implemented under the sub-project 3 of the project "Infrastructure of national research networks in the fields of Precision Medicine, Quantum Technology and Climate Change," funded by the Public Investment Program of Greece, General Secretary of Research and Technology/Ministry of Development and Investments." Researchers from GRC Geociències Marines benefited from a Grups de Recerca Consolidats grant (2017 SGR 315) by Generalitat de Catalunya autonomous government.

ACKNOWLEDGMENTS

We sincerely thank the officers, crews of *R/V* Aegaeo (HCMR), C. Pasqual, O. Veres, and P. Lopez- Fernandez for their precious help during cruises, and A. Rumín-Caparrós for his valuable inputs and comments on the currentmeter data. Additionally, we sincerely thank Giorgos Kouvarakis for his contribution with the Finokalia station data and the back-trajectory calculations. The authors gratefully acknowledge the NOAA Air Resources Laboratory (ARL) for the provision of the HYSPLIT transport and dispersion model and/or READY website (https://www.ready.noaa.gov) used in this publication. Elemental analyses were performed at the Scientific and Technological Centers of the University of Barcelona. We would like to thank the Editor Timothy Ferdelman and the reviewers Gerard Versteegh and Facundo Matias Barrera for their very constructive comments that helped significantly to improve the quality of this paper.

SUPPLEMENTARY MATERIAL

The Supplementary Material for this article can be found online at: https://www.frontiersin.org/articles/10.3389/feart.2021.591948/full#supplementary-material.

REFERENCES

Aboul-Kassim, T. A. T., and Simoneit, B. R. T. (1995). Petroleum hydrocarbon fingerprinting and sediment transport assessed by molecular biomarker and multivariate statistical analyses in the Eastern Harbour of Alexandria, Egypt. *Mar. Pollut. Bull.* 30, 63–73. doi:10.1016/0025-326X(94)00102-F

Agusti, S., González-Gordillo, J. I., Vaqué, D., Estrada, M., Cerezo, M. I., Salazar, G., et al. (2015). Ubiquitous healthy diatoms in the deep sea confirm deep carbon injection by the biological pump. *Nat. Commun.* 6, 7608. doi:10.1038/ncomms8608

Altabet, M. A. (1996). "Nitrogen and carbon isotopic traces of the source and transformation of particles in the deep sea," in *Particle flux in the ocean*. Editors V. Ttekkot, P. Schufer H. S., and P. J. Depetris (Hoboken: John Wiley & Sons Ltd), 155–184.

Altabet, M. A. (2001). Nitrogen isotopic evidence for micronutrient control of fractional NO_3^- utilization in the equatorial Pacific. *Limnol. Oceanogr.* 46, 368–380. doi:10.4319/lo.2001.46.2.0368

Amitai, Y., Lehahn, Y., Lazar, A., and Heifetz, E. (2010). Surface circulation of the eastern Mediterranean Levantine basin: insights from analyzing 14 years of satellite altimetry data. *J. Geophys. Res.* 115, C10058. doi:10.1029/2010JC006147

Antoine, D., Morel, A., and André, J.-M. (1995). Algal pigment distribution and primary production in the eastern Mediterranean as derived from coastal zone color scanner observations. *J. Geophys. Res.* 100, 16193–16209. doi:10.1029/95JC00466

Archer, D., Winguth, A., Lea, D., and Mahowald, N. (2000). What caused the glacial/interglacial atmospheric pCO_2 cycles?. *Rev. Geophys.* 38, 159–189. doi:10.1029/1999RG000066

Armstrong, R. A., Lee, C., Hedges, J. I., Honjo, S., and Wakeham, S. G. (2002). A new, mechanistic model for organic carbon fluxes in the ocean based on the quantitative association of POC with ballast minerals. *Deep Sea Res. Part II Top. Stud. Oceanogr.* 49, 219–236. doi:10.1016/S0967-0645(01)00101-1

Azov, Y (1991). Eastern Mediterranean—a marine desert?. *Mar. Pollut. Bull.* 23, 225–232.

Bach, L. T., Boxhammer, T., Larsen, A., Hildebrandt, N., Schulz, K. G., and Riebesell, U. (2016). Influence of plankton community structure on the sinking velocity of marine aggregates. *Global Biogeochem. Cycles* 30, 1145–1165. doi:10.1002/2016GB005372

Bar-Zeev, E., Berman, T., Rahav, E., Dishon, G., Herut, B., and Berman-Frank, I. (2011). Transparent exopolymer particle (TEP) dynamics in the Eastern Mediterranean Sea. *Mar. Ecol. Prog. Ser.* 431, 107–118. doi:10.3354/meps09110

Basu, S., Mackey, K. R. M., Basu, S., and Mackey, K. R. M. (2018). Phytoplankton as Key mediators of the biological carbon pump: their responses to a changing climate. *Sustainability* 10, 869. doi:10.3390/su10030869

Behrenfeld, M. J., and Falkowski, P. G. (1997). Photosynthetic rates derived from satellite-based chlorophyll concentration. *Limnol. Oceanogr.* 42, 1–20. doi:10.4319/lo.1997.42.1.0001

Belcher, A., Iversen, M., Giering, S., Riou, V., Henson, S. A., Berline, L., et al. (2016). Depth-resolved particle-associated microbial respiration in the northeast Atlantic. *Biogeosciences* 13, 4927–4943. doi:10.5194/bg-13-4927-2016

Bensi, M., Cardin, V., Rubino, A., Notarstefano, G., and Poulain, P. M. (2013). Effects of winter convection on the deep layer of the Southern Adriatic Sea in 2012. *J. Geophys. Res. Ocean.* 118, 6064–6075. doi:10.1002/2013JC009432

Blair, N. E., and Aller, R. C. (2012). The fate of terrestrial organic carbon in the marine environment. *Ann. Rev. Mar. Sci.* 4, 401–423. doi:10.1146/annurev-marine-120709-142717

Bosc, E., Bricaud, A., and Antoine, D. (2004). Seasonal and interannual variability in algal biomass and primary production in the Mediterranean Sea, as derived from 4 years of SeaWiFS observations. *Global Biogeochem. Cycles* 18, GB1005. doi:10.1029/2003GB002034

Bosc, E. (2004). Seasonal and interannual variability in algal biomass and primary production in the Mediterranean Sea, as derived from 4 years of SeaWiFS observations. *Global Biogeochem. Cycles* 18, GB1005. doi:10.1029/2003GB002034

Boyd, P. W., and Trull, T. W. (2007). Understanding the export of biogenic particles in oceanic waters: is there consensus?. *Prog. Oceanogr.* 72, 276–312. doi:10.1016/j.pocean.2006.10.007

Bressac, M., Guieu, C., Doxaran, D., Bourrin, F., Desboeufs, K., Leblond, N., et al. (2014). Quantification of the lithogenic carbon pump following a simulated dust-deposition event in large mesocosms. *Biogeosciences* 11, 1007–1020. doi:10.5194/bg-11-1007-2014

Browning, T. J., Stone, K., Bouman, H. A., Mather, T. A., Pyle, D. M., Moore, C. M., et al. (2015). Volcanic ash supply to the surface ocean-remote sensing of biological responses and their wider biogeochemical significance. *Front. Mar. Sci.* 2, 14. doi:10.3389/fmars.2015.00014

Buchan, A., LeCleir, G. R., Gulvik, C. A., and González, J. M. (2014). Master recyclers: features and functions of bacteria associated with phytoplankton blooms. *Nat. Rev. Microbiol.* 12, 686–698. doi:10.1038/nrmicro3326

Buesseler, K. O., and Boyd, P. W. (2009). Shedding light on processes that control particle export and flux attenuation in the twilight zone of the open ocean. *Limnol. Oceanogr.* 54, 1210–1232. doi:10.4319/lo.2009.54.4.1210

Buesseler, K. O. (1998). The decoupling of production and particulate export in the surface ocean. *Global Biogeochem. Cycles* 12, 297–310. doi:10.1029/97GB03366

Burdige, D. J. (2007). Preservation of organic matter in marine sediments: controls, mechanisms, and an imbalance in sediment organic carbon budgets?. *Chem. Rev.* 107, 467–485. doi:10.1021/cr050347q

Burkhardt, S., Riebesell, U., and Zondervan, I. (1999). Stable carbon isotope fractionation by marine phytoplankton in response to daylength, growth rate, and CO_2 availability. *Mar. Ecol. Prog. Ser.* 184, 31–41. doi:10.3354/meps184031

Cavan, E. L., Le Moigne, F. A. C., Poulton, A. J., Tarling, G. A., Ward, P., Daniels, C. J., et al. (2015). Attenuation of particulate organic carbon flux in the Scotia Sea, Southern Ocean, is controlled by zooplankton fecal pellets. *Geophys. Res. Lett.* 42, 821–830. doi:10.1002/2014GL062744

Christodoulaki, S., Petihakis, G., Kanakidou, M., Mihalopoulos, N., Tsiaras, K., and Triantafyllou, G. (2013). Atmospheric deposition in the Eastern Mediterranean. A driving force for ecosystem dynamics. *J. Mar. Syst.* 109–110, 78–93. doi:10.1016/j.jmarsys.2012.07.007

Christodoulou, S., Marty, J.-C., Miquel, J.-C., Volkman, J. K., and Rontani, J.-F. (2009). Use of lipids and their degradation products as biomarkers for carbon cycling in the northwestern Mediterranean Sea. *Mar. Chem.* 113, 25–40. doi:10.1016/j.marchem.2008.11.003

Close, H. G., Wakeham, S. G., and Pearson, A. (2014). Lipid and ^{13}C signatures of submicron and suspended particulate organic matter in the Eastern Tropical North Pacific: implications for the contribution of Bacteria. *Deep. Res. Part I* 85, 15–34. doi:10.1016/j.dsr.2013.11.005

Collister, J. W., Rieley, G., Stern, B., Eglinton, G., and Fry, B. (1994). Compound-specific δ13C analyses of leaf lipids from plants with differing carbon dioxide metabolisms. *Org. Geochem.* 21, 619–627. doi:10.1016/0146-6380(94)90008-6

Conte, M. H., Dickey, T. D., Weber, J. C., Johnson, R. J., and Knap, A. H. (2003). Transient physical forcing of pulsed export of bioreactive material to the deep Sargasso Sea. *Deep-Sea Res. Part I Oceanogr. Res. Pap.* 50, 1157–1187. doi:10.1016/S0967-0637(03)00141-9

Conte, M. H., Weber, J. C., and Ralph, N. (1998). Episodic particle flux in the deep Sargasso Sea. *Deep-Sea Res. Part I Oceanogr. Res. Pap.* 45, 1819–1841. doi:10.1016/S0967-0637(98)00046-6

Dagg, M. J., Jackson, G. A., and Checkley, D. M. (2014). The distribution and vertical flux of fecal pellets from large zooplankton in Monterey bay and coastal California. *Deep. Res. Part I Oceanogr. Res. Pap.* 94, 72–86. doi:10.1016/j.dsr.2014.09.001

Dauwe, B., and Middelburg, J. J. (1998). Amino acids and hexosamines as indicators of organic matter degradation state in North Sea sediments. *Limnol. Oceanogr.* 43, 782–798. doi:10.4319/lo.1998.43.5.0782

De Bar, M. W., Ullgren, J. E., Thunnell, R. C., Wakeham, S. G., Brummer, G. J. A., Stuut, J. B. W., et al. (2019). Long-chain diols in settling particles in tropical oceans: insights into sources, seasonality and proxies. *Biogeosciences* 16, 1705–1727. doi:10.5194/bg-16-1705-2019

De La Rocha, C. L., and Passow, U. (2007). Factors influencing the sinking of POC and the efficiency of the biological carbon pump. *Deep. Res. Part II Top. Stud. Oceanogr.* 54, 639–658. doi:10.1016/j.dsr2.2007.01.004

Deuser, W. G., Degens, E. T., and Guillard, R. R. L. (1968). Carbon isotope relationships between plankton and sea water. *Geochem. Cosmochim. Acta* 32, 657–660. doi:10.1016/0016-7037(68)90055-0

DeVries, T., Primeau, F., and Deutsch, C. (2012). The sequestration efficiency of the biological pump. *Geophys. Res. Lett.* 39, 114. doi:10.1029/2012GL051963

Deyme, R., Bouloubassi, I., Taphanel-Valt, M. H., Miquel, J. C., Lorre, A., Marty, J. C., et al. (2011). Vertical fluxes of aromatic and aliphatic hydrocarbons in the Northwestern Mediterranean Sea. *Environ. Pollut.* 159, 3681–3691. doi:10.1016/j.envpol.2011.07.017

Durrieu de Madron, X., Houpert, L., Puig, P., Sanchez-Vidal, A., Testor, P., Bosse, A., et al. (2013). Interaction of dense shelf water cascading and open-sea convection in the northwestern Mediterranean during winter 2012. *Geophys. Res. Lett.* 40, 1379–1385. doi:10.1002/grl.50331

Eglinton, G., and Hamilton, R. J. (1967). Leaf epicuticular waxes. *Science* 156, 1322–1335. doi:10.1126/science.156.3780.1322

Fabres, J., Calafat, A., Sanchez-Vidal, A., Canals, M., and Heussner, S. (2002). Composition and spatio-temporal variability of particle fluxes in the western Alboran Gyre, Mediterranean Sea. *J. Mar. Syst.* 33, 431–456. doi:10.1016/S0924-7963(02)00070-2

Farrington, J., and Takada, H. (2014). Persistent organic pollutants (POPs), polycyclic aromatic hydrocarbons (PAHs), and plastics: examples of the status, trend, and cycling of organic chemicals of environmental concern in the ocean. *Oceanography* 27, 196–213. doi:10.5670/oceanog.2014.23

Finkel, Z. V, Beardall, J., Flynn, K. J., Quigg, A., Rees, T. A. V, and Raven, J. A. (2010). Phytoplankton in a changing world: cell size and elemental stoichiometry. *J. Plankton Res.* 32, 119–137. doi:10.1093/plankt/fbp098

Fischer, G., and Wefer, G. (1996). "Long-term observation of particle fluxes in the eastern Atlantic: seasonality, changes of flux with depth and comparison with the sediment record," in *The South Atlantic: present and past circulation*. Editors G. Wefer, W. H. Berger, G. Siedler, and G. Webb (Berlin.: Springer-Verlag), 325–344.

Francois, R., Honjo, S., Krishfield, R., and Manganini, S. (2002). Factors controlling the flux of organic carbon to the bathypelagic zone of the ocean. *Global Biogeochem. Cycles* 16, 34–41. doi:10.1029/2001GB001722

Gelin, F., Boogers, I., Noordeloos, A. A. M., Damste, J. S. S., Riegman, R., and De Leeuw, J. W. (1997). Resistant biomacromolecules in marine microalgae of the classes Eustigmatophyceae and Chlorophyceae: geochemical implications. *Org. Geochem.* 26, 659–675. doi:10.1016/S0146-6380(97)00035-1

Giacomoni, P. P., Coltorti, M., Mollo, S., Ferlito, C., Braiato, M., and Scarlato, P. (2018). The 2011–2012 paroxysmal eruptions at Mt. Etna volcano: insights on the vertically zoned plumbing system. *J. Volcanol. Geoth. Res.* 349, 370–391. doi:10.1016/j.jvolgeores.2017.11.023

Goericke, R., and Fry, B. (1994). Variations of marine plankton δ13C with latitude, temperature, and dissolved CO_2 in the world ocean. *Global Biogeochem. Cycles* 8, 85–90. doi:10.1029/93GB03272

Gogou, A., Apostolaki, M., and Stephanou, E. G. (1998). Determination of organic molecular markers in marine aerosols and sediments: one-step flash chromatography compound class fractionation and capillary gas chromatographic analysis. *J. Chromatogr. A* 799, 215–231. doi:10.1016/S0021-9673(97)01106-0

Gogou, A., Bouloubassi, I., Lykousis, V., Arnaboldi, M., Gaitani, P., and Meyers, P. A. (2007). Organic geochemical evidence of late glacial–holocene climate instability in the north Aegean sea. *Palaeogeogr. Palaeoclimatol. Palaeoecol.* 256, 1–20. doi:10.1016/j.palaeo.2007.08.002

Gogou, A., Bouloubassi, I., and Stephanou, E. G. (2000). Marine organic geochemistry of the Eastern Mediterranean: 1. Aliphatic and polyaromatic hydrocarbons in Cretan Sea surficial sediments. *Mar. Chem.* 68, 265–282. doi:10.1016/S0304-4203(99)00082-1

Gogou, A., and Repeta, D. J. (2010). Particulate-dissolved transformations as a sink for semi-labile dissolved organic matter: chemical characterization of high molecular weight dissolved and surface-active organic matter in seawater and in diatom cultures. *Mar. Chem.* 121, 215–223. doi:10.1016/j.marchem.2010.05.001

Gogou, A., Sanchez-Vidal, A., Durrieu de Madron, X., Stavrakakis, S., Calafat, A., Stabholz, M., et al. (2014). Carbon flux to the deep in three open sites of the Southern European Seas (SES). *J. Mar. Syst.* 129, 224–233. doi:10.1016/j.jmarsys.2013.05.013

Gogou, A., and Stephanou, E. G. (2004). Marine organic geochemistry of the Eastern Mediterranean: 2. Polar biomarkers in Cretan Sea surficial sediments. *Mar. Chem.* 85, 1–25. doi:10.1016/j.marchem.2003.08.005

Goñi, M. A., and Hedges, J. I. (1995). Sources and reactivities of marine-derived organic matter in coastal sediments as determined by alkaline CuO oxidation. *Geochem. Cosmochim. Acta* 59, 2965–2981. doi:10.1016/0016-7037(95)00188-3

Goñi, M. A., Monacci, N., Gisewhite, R., Ogston, A., Crockett, J., and Nittrouer, C. (2006). Distribution and sources of particulate organic matter in the water column and sediments of the Fly River Delta, Gulf of Papua (Papua New Guinea). *Estuar. Coast Shelf Sci.* 69, 225–245. doi:10.1016/j.ecss.2006.04.012

Goñi, M. A., Teixeira, M. J., and Perkey, D. W. (2003). Sources and distribution of organic matter in a river-dominated estuary (Winyah Bay, SC, USA). *Estuar. Coast Shelf Sci.* 57, 1023–1048. doi:10.1016/S0272-7714(03)00008-8

Goñi, M. A., Yunker, M. B., Macdonald, R. W., and Eglinton, T. I. (2000). Distribution and sources of organic biomarkers in arctic sediments from the Mackenzie River and Beaufort Shelf. *Mar. Chem.* 71, 23–51. doi:10.1016/S0304-4203(00)00037-2

Gotsis-Skretas, O., Pagou, K., Moraitou-Apostolopoulou, M., and Ignatiades, L. (1999). Seasonal horizontal and vertical variability in primary production and standing stocks of phytoplankton and zooplankton in the Cretan Sea and the Straits of the Cretan Arc (March 1994-January 1995). *Prog. Oceanogr.* 44, 625–649. doi:10.1016/S0079-6611(99)00048-8

Gough, M. A., and Rowland, S. J. (1990). Characterization of unresolved complex mixtures of hydrocarbons in petroleum. *Nature* 344, 648–650. doi:10.1038/344648a0

Goutx, M., Momziko, A., Striby, L., Andersen, V., Marty, J. C., and Vescovali, I. (2000). High-frequency fluxes of labile compounds in the central Ligurian Sea. *Northwestern Mediterranean* 47, 3–4.

Goutx, M., Wakeham, S. G., Lee, C., Duflos, M., Guigue, C., Liu, Z., et al. (2007). Composition and degradation of marine particles with different settling velocities in the northwestern Mediterranean Sea. *Limnol. Oceanogr.* 52, 1645–1664. doi:10.4319/lo.2007.52.4.1645

Grice, K., Klein Breteler, W., Schouten, S., Grossi, V., de Leeuw, J. W., and Sinninghe-Damsté, J. S. (1998). Effects of zooplankton herbivory on biomarker proxy records. *Paleoceanography* 13, 686–693. doi:10.1029/98PA01871

Guidi, L., Stemmann, L., Jackson, G. A., Ibanez, F., Claustre, H., Legendre, L., et al. (2009). Effects of phytoplankton community on production, size, and export of large aggregates: a world-ocean analysis. *Limnol. Oceanogr.* 54, 1951–1963. doi:10.4319/lo.2009.54.6.1951

Harmelin-Vivien, M., Loizeau, V., Mellon, C., and Beker, B. (2008). Comparison of C and N stable isotope ratios between surface particulate organic matter and microphytoplankton in the Gulf of Lions (NW Mediterranean). *Continent. Shelf Res.* 28, 1911–1919. doi:10.1016/j.csr.2008.03.002

Harvey, H. R., O'Hara, S. C. M., Eglinton, G., and Corner, E. D. S. (1989). The comparative fate of dinosterol and cholesterol in copepod feeding: implications for a conservative molecular biomarker in the marine water column. *Org. Geochem.* 14, 635–641. doi:10.1016/0146-6380(89)90042-9

Hatzianestis, I., Parinos, C., Bouloubassi, I., and Gogou, A. (2020). Polycyclic aromatic hydrocarbons in surface sediments of the Aegean Sea (Eastern Mediterranean Sea). *Mar. Pollut. Bull.* 153, 111030. doi:10.1016/j.marpolbul.2020.111030

Hays, M. D. (2004). Nature of unresolved complex mixture in size-distributed emissions from residential wood combustion as measured by thermal desorption-gas chromatography-mass spectrometry. *J. Geophys. Res.* 109, D16S04. doi:10.1029/2003JD004051

Hedges, J. I., Keil, R. G., and Benner, R. (1997). What happens to terrestrial organic matter in the ocean?. *Org. Geochem.* 27, 195–212. doi:10.1016/S0146-6380(97)00066-1

Henley, S. F., Annett, A. L., Ganeshram, R. S., Carson, D. S., Weston, K., Crosta, X., et al. (2012). Factors influencing the stable carbon isotopic composition of suspended and sinking organic matter in the coastal Antarctic sea ice environment. *Biogeosciences* 9, 1137–1157. doi:10.5194/bg-9-1137-2012

Henson, S. A., Sanders, R., and Madsen, E. (2012). Global patterns in efficiency of particulate organic carbon export and transfer to the deep ocean. *Global Biogeochem. Cycles* 26, 33. doi:10.1029/2011GB004099

Henson, S. A., Yool, A., and Sanders, R. (2015). Variability in efficiency of particulate organic carbon export: a model study. *Global Biogeochem. Cycles* 29, 33–45. doi:10.1002/2014GB004965

Henson, S., Le Moigne, F., and Giering, S. (2019). Drivers of carbon export efficiency in the global ocean. *Global Biogeochem. Cycles* 33, 891–903. doi:10.1029/2018GB006158

Herndl, G. J., Agogué, H., Baltar, F., Reinthaler, T., Sintes, E., and Varela, M. (2008). Regulation of aquatic microbial processes: the 'microbial loop' of the sunlit

surface waters and the dark ocean dissected. *Aquat. Microb. Ecol.* 53, 59–68. doi:10.3354/ame01225

Herndl, G. J., and Reinthaler, T. (2013). Microbial control of the dark end of the biological pump. *Nat. Geosci.* 6, 718–724. doi:10.1038/ngeo1921

Heussner, S., Calafat, A., and Palanques, A. (1996). Quantitative and qualitative features of particle fluxes in *the north-balearic basin. EUROMARGE-NB final report*, Editors M. Canals, J. L. Casamor, I. Cacho, A. M. Calafat, and A. Monaco, (MAST II Program), 41–66.

Heussner, S., Ratti, C., and Carbonne, J. (1990). The PPS 3 time-series sediment trap and the trap sample processing techniques used during the ECOMARGE experiment. *Continent. Shelf Res.* 10, 943–958. doi:10.1016/0278-4343(90)90069-X

Hoefs, M. J. L., Rijpstra, W. I. C., and Damsté, J. S. S. (2002). The influence of oxic degradation on the sedimentary biomarker record I: evidence from Madeira Abyssal Plain turbidites. *Geochem. Cosmochim. Acta* 66, 2719–2735. doi:10.1016/S0016-7037(02)00864-5

Honjo, S., Manganini, S. J., Krishfield, R. a., and Francois, R. (2008). Particulate organic carbon fluxes to the ocean interior and factors controlling the biological pump: a synthesis of global sediment trap programs since 1983. *Prog. Oceanogr.* 76, 217–285. doi:10.1016/j.pocean.2007.11.003

Hu, J., Peng, P., Jia, G., Mai, B., and Zhang, G. (2006). Distribution and sources of organic carbon, nitrogen and their isotopes in sediments of the subtropical Pearl River estuary and adjacent shelf, Southern China. *Mar. Chem.* 98, 274–285. doi:10.1016/j.marchem.2005.03.008

Huertas, I. E., Ríos, A. F., García-Lafuente, J., Navarro, G., Makaoui, A., Sánchez-Román, A., et al. (2012). Atlantic forcing of the Mediterranean oligotrophy. *Global Biogeochem.* 26, 127. doi:10.1029/2011GB004167

Ignatiades, L., Gotsis-Skretas, O., Pagou, K., and Krasakopoulou, E. (2009). Diversification of phytoplankton community structure and related parameters along a large-scale longitudinal east–west transect of the Mediterranean Sea. *J. Plankton Res.* 31, 411–428. doi:10.1093/plankt/fbn124

Ioannou, A., Stegner, A., Le Vu, B., Taupier-Letage, I., and Speich, S. (2017). Dynamical evolution of ontense Ierapetra eddies on a 22 year long period. *J. Geophys. Res. Ocean.* 122, 9276–9298. doi:10.1002/2017JC013158

Israelevich, P., Ganor, E., Alpert, P., Kishcha, P., and Stupp, A. (2012). Predominant transport paths of saharan dust over the Mediterranean Sea to Europe. *J. Geophys. Res. Atmos.* 117, 33. doi:10.1029/2011JD016482

Janeković, I., Mihanović, H., Vilibić, I., and Tudor, M. (2014). Extreme cooling and dense water formation estimates in open and coastal regions of the Adriatic Sea during the winter of 2012. *J. Geophys. Res. Ocean.* 119, 3200–3218. doi:10.1002/2014JC009865

Jickells, T. D., An, Z. S., Andersen, K. K., Baker, A. R., Bergametti, G., Brooks, N., et al. (2005). Global iron connections between desert dust, ocean biogeochemistry, and climate. *Science* 308, 67–71. doi:10.1126/science.1105959

Kamatani, A., and Oku, O. (2000). Measuring biogenic silica in marine sediments. *Mar. Chem.* 68, 219–229. doi:10.1016/S0304-4203(99)00079-1

Kanakidou, M., Duce, R. A., Prospero, J. M., Baker, A. R., Benitez-Nelson, C., Dentener, F. J., et al. (2012). Atmospheric fluxes of organic N and P to the global ocean. *Global Biogeochem. Cycles* 26, 67. doi:10.1029/2011GB004277

Kanakidou, M., Mihalopoulos, N., Kindap, T., Im, U., Vrekoussis, M., Gerasopoulos, E., et al. (2011). Megacities as hot spots of air pollution in the East Mediterranean. *Atmos Environ* 45, 1223–1235. doi:10.1016/j.atmosenv.2010.11.048

Kanakidou, M., Myriokefalitakis, S., and Tsagkaraki, M. (2020). Atmospheric inputs of nutrients to the Mediterranean Sea. *Deep. Res. Part II Top. Stud. Oceanogr.* 171, 104606. doi:10.1016/j.dsr2.2019.06.014

Karageorgis, A. P., Kontoyiannis, H., Stavrakakis, S., Krasakopoulou, E., Gogou, A., Papadopoulos, A., et al. (2018). Particle dynamics and fluxes in canyons and open slopes of the southern Cretan margin (Eastern Mediterranean). *Prog. Oceanogr.* 169, 33–47. doi:10.1016/j.pocean.2017.12.009

Karl, D. M., Church, M. J., Dore, J. E., Letelier, R. M., and Mahaffey, C. (2012). Predictable and efficient carbon sequestration in the North Pacific Ocean supported by symbiotic nitrogen fixation. *Proc. Natl. Acad. Sci. U. S. A* 109, 1842–1849. doi:10.1073/pnas.1120312109

Kerhervé, P., Heussner, S., Charrière, B., Stavrakakis, S., Ferrand, J.-L., Monaco, A., et al. (1999). Biogeochemistry and dynamics of settling particle fluxes at the Antikythira strait (eastern mediterranean). *Prog. Oceanogr.* 44, 651–675. doi:10.1016/S0079-6611(99)00040-3

Kerhervé, P., Minagawa, M., Heussner, S., and Monaco, A. (2001). Stable isotopes ($^{13}C/^{12}C$ and $^{15}N/^{14}N$) in settling organic matter of the northwestern Mediterranean Sea: biogeochemical implications. *Oceanol. Acta* 24, 77–85. doi:10.1016/s0399-1784(00)01111-7

Klaas, C., and Archer, D. E. (2002). Association of sinking organic matter with various types of mineral ballast in the deep sea: implications for the rain ratio. *Global Biogeochem. Cycles* 16, 63–71. doi:10.1029/2001GB001765

Koppelmann, R., Weikert, H., Halsband-Lenk, C., and Jennerjahn, T. (2004). Mesozooplankton community respiration and its relation to particle flux in the oligotrophic eastern Mediterranean. *Global Biogeochem.* 18, 64. doi:10.1029/2003GB002121

Kouvarakis, G., Mihalopoulos, N., Tselepides, A., and Stavrakakis, S. (2001). On the importance of atmospheric inputs of inorganic nitrogen species on the productivity of the Eastern Mediterranean Sea. *Global Biogeochem. Cycles* 15, 805–817. doi:10.1029/2001GB001399

Krom, M. D., Herut, B., and Mantoura, R. F. C. (2004). Nutrient budget for the eastern mediterranean: implications for phosphorus limitation. *Limnol. Oceanogr.* 49, 1582–1592. doi:10.4319/lo.2004.49.5.1582

Krom, M. D., Kress, N., Brenner, S., and Gordon, L. I. (1991). Phosphorus limitation of primary productivity in the Eastern Mediterranean Sea. *Limnol. Oceanogr.* 36, 424–432. doi:10.4319/lo.1991.36.3.0424

Kubilay, N., Nickovic, S., Moulin, C., and Dulac, F. (2000). An illustration of the transport and deposition of mineral dust onto the eastern Mediterranean. *AtmosEnviron* 34, 1293–1303. doi:10.1016/S1352-2310(99)00179-X

Kwon, E. Y., Primeau, F., and Sarmiento, J. L. (2009). The impact of remineralization depth on the air–sea carbon balance. *Nat. Geosci.* 2, 630–635. doi:10.1038/ngeo612

Lampadariou, N., Tselepides, A., and Hatziyanni, E. (2009). Deep-sea meiofaunal and foraminiferal communities along a gradient of primary productivity in the Eastern Mediterranean Sea. *Sci. Mar.* 73, 337–345. doi:10.3989/scimar.2009.73n2337

Larnicol, G., Ayoub, N., and Le Traon, P. Y. (2002). Major changes in Mediterranean sea level variability from 7 years of TOPEX/Poseidon and ERS-1/2 data. *J. Mar. Syst.* 33–34, 63–89. doi:10.1016/S0924-7963(02)00053-2

Le Moigne, F. A. C., Henson, S. A., Cavan, E., Georges, C., Pabortsava, K., Achterberg, E. P., et al. (2016). What causes the inverse relationship between primary production and export efficiency in the Southern Ocean?. *Geophys. Res. Lett.* 43, 4457–4466. doi:10.1002/2016GL068480

Le Moigne, F. A. C., Poulton, A. J., Henson, S. A., Daniels, C. J., Fragoso, G. M., Mitchell, E., et al. (2015). Carbon export efficiency and phytoplankton community composition in the Atlantic sector of the Arctic Ocean. *J. Geophys. Res. Ocean.* 120, 3896–3912. doi:10.1002/2015JC010700

Lehmann, M. F., Bernasconi, S. M., Barbieri, A., and McKenzie, J. A. (2002). Preservation of organic matter and alteration of its carbon and nitrogen isotope composition during simulated and *in situ* early sedimentary diagenesis. *Geochem. Cosmochim. Acta* 66, 3573–3584. doi:10.1016/S0016-7037(02)00968-7

Lelieveld, J., Berresheim, H., Borrmann, S., Crutzen, P. J., Dentener, F. J., Fischer, H., et al. (2002). Global air pollution crossroads over the Mediterranean. *Science 84* 298, 794–799. doi:10.1126/science.1075457

Lewis, M. R., Hebert, D., Harrison, W. G., Platt, T., and Oakey, N. S. (1986). Vertical nitrate fluxes in the oligotrophic ocean. *Science* 234, 870–873. doi:10.1126/science.234.4778.870

Lima, I. D., Lam, P. J., and Doney, S. C. (2014). Dynamics of particulate organic carbon flux in a global ocean model. *Biogeosciences* 11, 1177–1198. doi:10.5194/bg-11-1177-2014

Lomas, M. W., Bates, N. R., Johnson, R. J., Knap, A. H., Steinberg, D. K., and Carlson, C. A. (2013). Two decades and counting: 24-years of sustained open ocean biogeochemical measurements in the Sargasso Sea. *Deep Sea Res. Part II Top. Stud. Oceanogr.* 93, 16–32. doi:10.1016/J.DSR2.2013.01.008

Longhurst, A., Sathyendranath, S., Platt, T., and Caverhill, C. (1995). An estimate of global primary production in the ocean from satellite radiometer data. *J. Plankton Res.* 17, 1245–1271. doi:10.1093/plankt/17.6.1245

Maiti, K., Charette, M. A., Buesseler, K. O., and Kahru, M. (2013). An inverse relationship between production and export efficiency in the Southern Ocean. *Geophys. Res. Lett.* 40, 1557–1561. doi:10.1002/grl.50219

Malinverno, E., Ziveri, P., and Corselli, C. (2003). Coccolithophorid distribution in the Ionian Sea and its relationship to eastern Mediterranean circulation during

late fall to early winter 1997. *J. Geophys. Res. C Oceans* 108, 33. doi:10.1029/2002jc001346

Malviya, S., Scalco, E., Audic, S., Vincent, F., Veluchamy, A., Poulain, J., et al. (2016). Insights into global diatom distribution and diversity in the world's ocean. *Proc. Natl. Acad. Sci. U. S. A* 113, E1516–E1525. doi:10.1073/pnas.1509523113

Marañón, E., Behrenfeld, M. J., González, N., Mouriño, B., and Zubkov, M. V. (2003). High variability of primary production in oligotrophic waters of the Atlantic Ocean: uncoupling from phytoplankton biomass and size structure. *Mar. Ecol. Prog. Ser.* 257, 1–11. doi:10.3354/meps257001

Marañón, E., Fernández, A., Mouriño-Carballido, B., MartÍnez-GarcÍa, S., Teira, E., Cermeño, P., et al. (2010). Degree of oligotrophy controls the response of microbial plankton to Saharan dust. *Limnol. Oceanogr.* 55, 2339–2352. doi:10.4319/lo.2010.55.6.2339

Marchand, D., Marty, J. C., Miquel, J. C., and Rontani, J. F. (2005). Lipids and their oxidation products as biomarkers for carbon cycling in the northwestern Mediterranean Sea: results from a sediment trap study. *Mar. Chem.* 95, 129–147. doi:10.1016/j.marchem.2004.09.001

Marlowe, I. T., Green, J. C., Neal, A. C., Brassell, S. C., Eglinton, G., and Course, P. A. (1984). Long chain (*n*-C37–C39) alkenones in the Prymnesiophyceae. Distribution of alkenones and other lipids and their taxonomic significance. *Br. Phycol. J.* 19, 203–216. doi:10.1080/00071618400650221

Marty, J. C., Goutx, M., Guigue, C., Leblond, N., Raimbault, P., Villefranche, D., et al. (2009). Short-term changes in particulate fluxes measured by drifting sediment traps during end summer oligotrophic regime in the NW Mediterranean Sea. *Biogeosciences* 6, 887–899. doi:10.5194/bg-6-887-2009

Masqué, P., Fabres, J., Canals, M., Sanchez-Cabeza, J. A., Sanchez-Vidal, A., Cacho, I., et al. (2003). Accumulation rates of major constituents of hemipelagic sediments in the deep Alboran Sea: a centennial perspective of sedimentary dynamics. *Mar. Geol.* 193, 207–233. doi:10.1016/S0025-3227(02)00593-5

Meador, T. B., Gogou, A., Spyres, G., Herndl, G. J., Krasakopoulou, E., Psarra, S., et al. (2010). Biogeochemical relationships between ultrafiltered dissolved organic matter and picoplankton activity in the Eastern Mediterranean Sea. *Deep Sea Res. Part II Top. Stud. Oceanogr.* 57, 1460–1477. doi:10.1016/j.dsr2.2010.02.015

Meglen, R. R. (1992). Examining large databases: a chemometric approach using principal component analysis. *Mar. Chem.* 39, 217–237.

Méjanelle, L., and Dachs, J. (2009). Short scale (6 h) temporal variation of sinking fluxes of planktonic and terrigeneous lipids at 200 m in the NW Mediterranean Sea. *Biogeosciences* 6, 3017–3034. doi:10.5194/bg-6-3017-2009

Meyers, P. A. (1997). Organic geochemical proxies of paleoceanographic, paleolimnologic, and paleoclimatic processes. *Org. Geochem.* 27, 213–250. doi:10.1016/S0146-6380(97)00049-1

Meyers, P. A. (1994). Preservation of elemental and isotopic source identification of sedimentary organic matter. *Chem. Geol.* 114, 289–302. doi:10.1016/0009-2541(94)90059-0

Mihalopoulos, N., Stephanou, E., Kanakidou, M., Pilitsidis, S., and Bousquet, P. (1997). Tropospheric aerosol ionic composition in the Eastern Mediterranean region. *Tellus Ser. B Chem. Phys. Meteorol.* 49, 314–326. doi:10.3402/tellusb.v49i3.15970

Mkhinini, N., Coimbra, A. L. S., Stegner, A., Arsouze, T., Taupier-Letage, I., and Béranger, K. (2014). Long-lived mesoscale eddies in the Eastern Mediterranean Sea: analysis of 20 years of AVISO geostrophic velocities. *J. Geophys. Res. Ocean.* 119, 8603–8626. doi:10.1002/2014JC010176

Mortlock, R. A., and Froelich, P. N. (1989). A simple method for the rapid determination of biogenic opal in pelagic marine sediments. *Deep Sea Res. Part A. Oceanogr. Res. Pap.* 36, 1415–1426. doi:10.1016/0198-0149(89)90092-7

Moulin, C., Lambert, C. E., Dayan, U., Masson, V., Ramonet, M., Bousquet, P., et al. (1998). Satellite climatology of African dust transport in the Mediterranean atmosphere. *J. Geophys. Res. Atmos.* 103, 13137–13144. doi:10.1029/98JD00171

Moutin, T., and Raimbault, P. (2002). Primary production, carbon export and nutrients availability in western and Eastern Mediterranean Sea in early summer 1996 (MINOS cruise). *J. Mar. Syst.* 33–34, 273–288. doi:10.1016/S0924-7963(02)00062-3

Nakanishi, T., and Minagawa, M. (2003). Stable carbon and nitrogen isotopic compositions of sinking particles in the northeast Japan Sea. *Geochem. J.* 37, 261–275. doi:10.2343/geochemj.37.261

Napolitano, E., Oguz, T., Malanotte-Rizzoli, P., Yilmaz, A., and Sansone, E. (2000). Simulations of biological production in the Rhodes and Ionian basins of the eastern Mediterranean. *J. Mar. Syst.* 24, 277–298. doi:10.1016/S0924-7963(99)00090-1

Neal, A. C., Prahl, F. G., Eglinton, G., O'Hara, S. C. M., and Corner, E. D. S. (1986). Lipid changes during a planktonic feeding sequence involving unicellular algae, *Elminius nauplii* and adult *Calanus*. *J. Mar. Biol. Assoc. U. K.* 66, 1. doi:10.1017/S0025315400039606

Nieuwenhuize, J., Maas, Y. E. M., and Middelburg, J. J. (1994). Rapid analysis of organic carbon and nitrogen in particulate materials. *Mar. Chem.* 45, 217–224. doi:10.1016/0304-4203(94)90005-1

Ohkouchi, N., Kawamura, K., Kawahata, H., and Taira, A. (1997). Latitudinal distributions of terrestrial biomarkers in the sediments from the Central Pacific. *Geochem. Cosmochim. Acta* 61, 1911–1918. doi:10.1016/S0016-7037(97)00040-9

Olgun, N., Duggen, S., Andronico, D., Kutterolf, S., Croot, P. L., Giammanco, S., et al. (2013). Possible impacts of volcanic ash emissions of Mount Etna on the primary productivity in the oligotrophic Mediterranean Sea: results from nutrient-release experiments in seawater. *Mar. Chem.* 152, 32–42. doi:10.1016/j.marchem.2013.04.004

Ortega-Retuerta, E., Mazuecos, I. P., Reche, I., Gasol, J. M., Álvarez-Salgado, X. A., Álvarez, M., et al. (2019). Transparent exopolymer particle (TEP) distribution and *in situ* prokaryotic generation across the deep Mediterranean Sea and nearby North East Atlantic Ocean. *Prog. Oceanogr.* 173, 180–191. doi:10.1016/j.pocean.2019.03.002

Palanques, A., and Puig, P. (2018). Particle fluxes induced by benthic storms during the 2012 dense shelf water cascading and open sea convection period in the northwestern Mediterranean basin. *Mar. Geol.* 406, 119–131. doi:10.1016/j.margeo.2018.09.010

Parinos, C., Gogou, A., Bouloubassi, I., Pedrosa-Pàmies, R., Hatzianestis, I., Sanchez-Vidal, A., et al. (2013a). Occurrence, sources and transport pathways of natural and anthropogenic hydrocarbons in deep-sea sediments of the Eastern Mediterranean Sea. *Biogeosciences* 10, 6069–6089. doi:10.5194/bg-10-6069-2013

Parinos, C., Gogou, A., Bouloubassi, I., Stavrakakis, S., Plakidi, E., and Hatzianestis, I. (2013b). Sources and downward fluxes of polycyclic aromatic hydrocarbons in the open southwestern Black Sea. *Org. Geochem.* 57, 65–75. doi:10.1016/j.orggeochem.2013.01.007

Parinos, C., Gogou, A., Krasakopoulou, E., Lagaria, A., Giannakourou, A., Karageorgis, A. P., et al. (2017). Transparent exopolymer particles (TEP) in the NE Aegean sea frontal area: seasonal dynamics under the influence of black sea water. *Continent. Shelf Res.* 149, 112–123. doi:10.1016/j.csr.2017.03.012

Parinos, C., and Gogou, A. (2016). Suspended particle-associated PAHs in the open Eastern Mediterranean Sea: occurrence, sources and processes affecting their distribution patterns. *Mar. Chem.* 180, 42–50. doi:10.1016/j.marchem.2016.02.001

Pasqual, C., Calafat, A., Lopez-Fernandez, P., and Pusceddu, A. (2015). Organic carbon inputs to the sea bottom of the Mallorca continental slope. *J. Mar. Syst.* 148, 142–151. doi:10.1016/j.jmarsys.2015.02.006

Passow, U., and De La Rocha, C. L. (2006). Accumulation of mineral ballast on organic aggregates. *Global Biogeochem. Cycles* 20, 17. doi:10.1029/2005GB002579

Passow, U. (2002a). Production of transparent exopolymer particles (TEP) by phyto- and bacterioplankton. *Mar. Ecol. Prog. Ser.* 236, 1–12. doi:10.3354/meps236001

Passow, U. (2002b). Transparent exopolymer particles (TEP) in aquatic environments. *Prog. Oceanogr.* 55, 287–333. doi:10.1016/S0079-6611(02)00138-6

Patara, L., Pinardi, N., Corselli, C., Malinverno, E., Tonani, M., Santoleri, R., et al. (2009). Particle fluxes in the deep Eastern Mediterranean basins: the role of ocean vertical velocities. *Biogeosciences* 6, 29. doi:10.5194/bg-6-333-2009

Pavlidou, A., Velaoras, D., Karageorgis, A. P., Rousselaki, E., Parinos, C., Dähnke, K., et al. (2020). Seasonal variations of biochemical and optical properties, physical dynamics and N stable isotopic composition in three northeastern Mediterranean basins (Aegean, Cretan and Ionian Seas). *Deep. Res. Part II Top. Stud. Oceanogr.* 171, 104704. doi:10.1016/j.dsr2.2019.104704

Pedrosa-Pàmies, R., Conte, M. H., Weber, J. C., and Johnson, R. (2018). Carbon cycling in the Sargasso Sea water column: insights from lipid biomarkers in

suspended particles. *Prog. Oceanogr.* 168, 248–278. doi:10.1016/J.POCEAN.2018.08.005

Pedrosa-Pàmies, R., Conte, M. H., Weber, J. C., and Johnson, R. (2019). Hurricanes enhance labile carbon export to the deep ocean. *Geophys. Res. Lett.* 46, 10484–10494. doi:10.1029/2019GL083719

Pedrosa-Pàmies, R., Parinos, C., Sanchez-Vidal, A., Gogou, A., Calafat, A., Canals, M., et al. (2015). Composition and sources of sedimentary organic matter in the deep Eastern Mediterranean Sea. *Biogeosciences* 12, 7379–7402. doi:10.5194/bgd-12-9935-2015

Pedrosa-Pàmies, R., Sanchez-Vidal, A., Calafat, A., Canals, M., and Durán, R. (2013). Impact of storm-induced remobilization on grain size distribution and organic carbon content in sediments from the Blanes Canyon area, NW Mediterranean Sea. *Prog. Oceanogr.* 118, 122–136. doi:10.1016/j.pocean.2013.07.023

Pedrosa-Pàmies, R., Sanchez-Vidal, A., Canals, M., Lampadariou, N., Velaoras, D., Gogou, A., et al. (2016). Enhanced carbon export to the abyssal depths driven by atmosphere dynamics. *Geophys. Res. Lett.* 43, 8626–8636. doi:10.1002/2016GL069781

Perdue, E. M., and Koprivnjak, J.-F. (2007). Using the C/N ratio to estimate terrigenous inputs of organic matter to aquatic environments. *Estuar. Coast Shelf Sci.* 73, 65–72. doi:10.1016/j.ecss.2006.12.021

Prahl, F. G., Eglinton, G., Corner, E. D. S., O'Hara, S. C. M., and Forsberg, T. E. V. (1984). Changes in plant lipids during passage through the gut of Calanus. *J. Mar. Biol. Assoc. U. K.* 64, 317. doi:10.1017/S0025315400030022

Psarra, S., Tselepides, A., and Ignatiades, L. (2000). Primary productivity in the oligotrophic Cretan Sea (NE Mediterranean): seasonal and interannual variability. *Prog. Oceanogr.* 46, 187–204. doi:10.1016/S0079-6611(00)00018-5

Puigcorbé, V., Benitez-Nelson, C. R., Masqué, P., Verdeny, E., White, A. E., Popp, B. N., et al. (2015). Small phytoplankton drive high summertime carbon and nutrient export in the Gulf of California and Eastern Tropical North Pacific. *Global Biogeochem. Cycles* 29, 1309–1332. doi:10.1002/2015GB005134

Quirós-Collazos, L., Pedrosa-Pàmies, R., Sanchez-Vidal, A., Guillén, J., Duran, R., and Cabelloa, P. (2017). Distribution and sources of organic matter in size-fractionated nearshore sediments off the Barcelona city (NW Mediterranean). *Estuar. Coast Shelf Sci.* 189, 47. doi:10.1016/j.ecss.2017.03.004

Rampen, S. W., Willmott, V., Kim, J.-H., Uliana, E., Mollenhauer, G., Schefuß, E., et al. (2012). Long chain 1,13- and 1,15-diols as a potential proxy for palaeotemperature reconstruction. *Geochem. Cosmochim. Acta* 84, 201–216. doi:10.1016/j.gca.2012.01.024

Rau, G. H., Takahashi, T., Des Marais, D. J., Repeta, D. J., and Martin, J. H. (1992). The relationship between $\delta^{13}C$ of organic matter and $[CO_2(aq)]$ in ocean surface water: data from a JGOFS site in the northeast Atlantic Ocean and a model. *Geochem. Cosmochim. Acta* 56, 1413–1419. doi:10.1016/0016-7037(92)90073-R

Raveh, O., David, N., Rilov, G., and Rahav, E. (2015). The temporal dynamics of coastal phytoplankton and bacterioplankton in the Eastern Mediterranean Sea. *PloS One* 10, e0140690. doi:10.1371/journal.pone.0140690

Raven, J. A. (1998). The twelfth Tansley Lecture. Small is beautiful: the picophytoplankton. *Funct. Ecol.* 12, 503–513. doi:10.1046/j.1365-2435.1998.00233.x

Redfield, A. C., Ketchum, B. H., and Richards, F. A. (1963). "The influence of organisms on the composition of sea-water," in *The Sea*. Editor M. N. Hill (New York: Interscience), 26–77.

Reemtsma, T., and Ittekkot, V. (1992). Determination of factors controlling the fatty acid composition of settling particles in the water column by principal-component analysis and their quantitative assessment by multiple regression. *Org. Geochem.* 18, 121–129. doi:10.1016/0146-6380(92)90149-R

Ribera d'Alcalà, M. (2003). Nutrient ratios and fluxes hint at overlooked processes in the Mediterranean Sea. *J. Geophys. Res.* 108, 8106. doi:10.1029/2002JC001650

Robinson, A. R., and Golnaraghi, M. (1993). Circulation and dynamics of the Eastern Mediterranean Sea; quasi-synoptic data-driven simulations. *Deep Sea Res. Part II Top. Stud. Oceanogr.* 40, 1207–1246. doi:10.1016/0967-0645(93)90068-X

Rolph, G., Stein, A., and Stunder, B. (2017). Real-time environmental Applications and display sYstem: READY. *Environ. Model. Software* 95, 210–228. doi:10.1016/j.envsoft.2017.06.025

Rumolo, P., Barra, M., Gherardi, S., Marsella, E., and Sprovieri, M. (2011). Stable isotopes and C/N ratios in marine sediments as a tool for discriminating anthropogenic impact. *J. Environ. Monit.* 13, 3399–3408. doi:10.1039/c1em10568j

Sanchez-Vidal, A., Calafat, A., Canals, M., Frigola, J., and Fabres, J. (2005). Particle fluxes and organic carbon balance across the eastern Alboran Sea (SW Mediterranean Sea). *Continent. Shelf Res.* 25, 609–628. doi:10.1016/j.csr.2004.11.004

Sanchez-Vidal, A., Higueras, M., Martí, E., Liquete, C., Calafat, A., and Kerhervé, P. (2013). Riverine transport of terrestrial organic matter to the North Catalan margin, NW Mediterranean Sea. *Prog. Oceanogr.* 118, 71–80. doi:10.1016/j.pocean.2013.07.020

Sanchez-Vidal, A., Pasqual, C., Kerhervé, P., Calafat, A., Heussner, S., Palanques, A., et al. (2008). Impact of dense shelf water cascading on the transfer of organic matter to the deep western Mediterranean basin. *Geophys. Res. Lett.* 35, L05605. doi:10.1029/2007GL032825

Schneider, J. K., Gagosian, R. B., Cochran, J. K., and Trull, T. W. (1983). Particle size distributions of n-alkanes and 210Pb in aerosols off the coast of Peru. *Nature* 304, 429–432. doi:10.1038/304429a0

Sciare, J., Bardouki, H., Moulin, C., and Mihalopoulos, N. (2003). Aerosol sources and their contribution to the chemical composition of aerosols in the Eastern Mediterranean Sea during summertime. *Atmos. Chem. Phys.* 3, 291–302. doi:10.5194/acp-3-291-2003

Scollo, S., Prestifilippo, M., Pecora, E., Corradini, S., Merucci, L., Spata, G., et al. (2014). Eruption column height estimation of the 2011-2013 Etna lava fountains. *Ann. Geophys.* 57, S0214. doi:10.4401/ag-6396

Sempéré, R., Yoro, S., Van Wambeke, F., and Charrière, B. (2000). Microbial decomposition of large organic particles in the northwestern Mediterranean Sea: an experimental approach. *Mar. Ecol. Prog. Ser.* 198, 61–72. doi:10.3354/meps198061

Sheridan, C. C., Lee, C., Wakeham, S. G., and Bishop, J. K. B. (2002). Suspended particle organic composition and cycling in surface and midwaters of the equatorial Pacific Ocean. *Deep-Sea Res. Part I Oceanogr. Res. Pap.* 49, 1983–2008. doi:10.1016/S0967-0637(02)00118-8

Simoneit, B. R. T., Cardoso, J. N., and Robinson, N. (1990). An assessment of the origin and composition of higher molecular weight organic matter in aerosols over Amazonia. *Chemosphere* 21, 1285–1301. doi:10.1016/0045-6535(90)90145-J

Simoneit, B. R. T. (1984). Organic matter of the troposphere-III. Characterization and sources of petroleum and pyrogenic residues in aerosols over the western United States. *Atmos. Environ.* 18, 51–67. doi:10.1016/0004-6981(84)90228-2

Siokou-Frangou, I., Bianchi, M., Christaki, U., Christou, E. D., Giannakourou, A., Gotsis, O., et al. (2002). Carbon flow in the planktonic food web along a gradient of oligotrophy in the Aegean Sea (Mediterranean Sea). *J. Mar. Syst.* 33–34, 335–353. doi:10.1016/S0924-7963(02)00065-9

Siokou-Frangou, I., Christaki, U., Mazzocchi, M. G., Montresor, M., Ribera d'Alcalá, M., Vaqué, D., et al. (2010). Plankton in the open Mediterranean Sea: a review. *Biogeosciences* 7, 1543–1586. doi:10.5194/bg-7-1543-2010

Siokou-Frangou, I., Gotsis-Skretas, O., Christou, E. D., and Pagou, K. (1999). *The eastern Mediterranean as a laboratory Basin for the Assessment of contrasting ecosystems*. Berlin: Springer Netherlands, 205–223. doi:10.1007/978-94-011-4796-5_15Plankton characteristics in the Aegean, ionian and NW Levantine seas

Skampa, E., Triantaphyllou, M. V., Dimiza, M. D., Gogou, A., Malinverno, E., Stavrakakis, S., et al. (2020). Coccolithophore export in three deep-sea sites of the Aegean and Ionian Seas (Eastern Mediterranean): biogeographical patterns and biogenic carbonate fluxes. *Deep. Res. Part II Top. Stud. Oceanogr.* 171, 104690. doi:10.1016/j.dsr2.2019.104690

Skampa, E., Triantaphyllou, M. V., Dimiza, M. D., Gogou, A., Malinverno, E., Stavrakakis, S., et al. (2019). Coupling plankton—sediment trap—surface sediment coccolithophore regime in the North Aegean Sea (NE Mediterranean). *Mar. Micropaleontol.* 152, 101729. doi:10.1016/j.marmicro.2019.03.001

Smith, K. L., Ruhl, H. A., Bett, B. J., Billett, D. S. M., Lampitt, R. S., and Kaufmann, R. S. (2009). Climate, carbon cycling, and deep-ocean ecosystems. *Proc. Natl. Acad. Sci. U. S. A* 106, 19211. doi:10.1073/pnas.0908322106–8

Smith, K. L., Ruhl, H. A., Huffard, C. L., Messié, M., and Kahru, M. (2018). Episodic organic carbon fluxes from surface ocean to abyssal depths during long-term monitoring in NE Pacific. *Proc. Natl. Acad. Sci. U. S. A.* 115, 12235–12240. doi:10.1073/PNAS.1814559115

Stabholz, M., Durrieu de Madron, X., Canals, M., Khripounoff, A., Taupier-Letage, I., Testor, P., et al. (2013). Impact of open-ocean convection on particle fluxes and sediment dynamics in the deep margin of the Gulf of Lions. *Biogeosciences* 10, 1097–1116. doi:10.5194/bg-10-1097-2013

Stavrakakis, S., Chronis, G., Tselepides, A., Heussner, S., Monaco, A., and Abassi, A. (2000). Downward fluxes of settling particles in the deep Cretan Sea (NE Mediterranean). *Prog. Oceanogr.* 46, 217–240. doi:10.1016/S0079-6611(00)00020-3

Stavrakakis, S., Gogou, A., Krasakopoulou, E., Karageorgis, A. P., Kontoyiannis, H., Rousakis, G., et al. (2013). Downward fluxes of sinking particulate matter in the deep Ionian Sea (NESTOR site), eastern Mediterranean: seasonal and interannual variability. *Biogeosciences* 10, 7235–7254. doi:10.5194/bg-10-7235-2013

Stein, A. F., Draxler, R. R., Rolph, G. D., Stunder, B. J. B., Cohen, M. D., and Ngan, F. (2015). Noaa's hysplit atmospheric transport and dispersion modeling system. *Bull. Am. Meteorol. Soc.* 96, 2059–2077. doi:10.1175/BAMS-D-14-00110.1

Steinberg, D. K., Carlson, C. A., Bates, N. R., Johnson, R. J., Michaels, A. F., and Knap, A. H. (2001). Overview of the US JGOFS Bermuda Atlantic Time-series Study (BATS): a decade-scale look at ocean biology and biogeochemistry. *Deep Sea Res. Part II Top. Stud. Oceanogr.* 48, 1405–1447. doi:10.1016/S0967-0645(00)00148-X

Steinberg, D. K., Goldthwait, S. A., and Hansell, D. A. (2002). Zooplankton vertical migration and the active transport of dissolved organic and inorganic nitrogen in the Sargasso Sea. *Deep. Res. Part I Oceanogr. Res. Pap.* 49, 1445–1461. doi:10.1016/S0967-0637(02)00037-7

Struck, U., Pollehne, F., Bauerfeind, E., and Bodungen, B. V. (2004). Sources of nitrogen for the vertical particle flux in the Gotland Sea (Baltic Proper) - results from sediment trap studies. *J. Mar. Syst.* 45, 91–101. doi:10.1016/j.jmarsys.2003.11.012

Teshima, S.-I. (1971). Bioconversion of β-sitosterol and 24-methylcholesterol to cholesterol in marine crustacea. *Comp. Biochem. Physiol. Part B Comp. Biochem.* 39, 815–822. doi:10.1016/0305-0491(71)90105-2

Tesi, T., Puig, P., Palanques, A., and Goñi, M. A. (2010). Lateral advection of organic matter in cascading-dominated submarine canyons. *Prog. Oceanogr.* 84, 185–203. doi:10.1016/j.pocean.2009.10.004

Theodosi, C., Markaki, Z., Pantazoglou, F., Tselepides, A., and Mihalopoulos, N. (2019). Chemical composition of downward fluxes in the Cretan Sea (Eastern Mediterranean) and possible link to atmospheric deposition: a 7 year survey. *Deep. Res. Part II Top. Stud. Oceanogr.* 164, 89–99. doi:10.1016/j.dsr2.2019.06.003

Theodosi, C., Parinos, C., Gogou, A., Kokotos, A., Stavrakakis, S., Lykousis, V., et al. (2013). Downward fluxes of elemental carbon, metals and polycyclic aromatic hydrocarbons in settling particles from the deep Ionian Sea (NESTOR site), Eastern Mediterranean. *Biogeosciences* 10, 4449–4464. doi:10.5194/bg-10-4449-2013

Thunell, R. C., Varela, R., Llano, M., Collister, J., -Karger, F. M., and Bohrer, R. (2000). Organic carbon fluxes, degradation, and accumulation in an anoxic basin: sediment trap results from the Cariaco Basin. *Limnol. Oceanogr.* 45, 300–308. doi:10.4319/lo.2000.45.2.0300

Tolosa, I., LeBlond, N., Copin-Montégut, C., Marty, J.-C., de Mora, S., and Prieur, L. (2003). Distribution of sterol and fatty alcohol biomarkers in particulate matter from the frontal structure of the Alboran Sea (S.W. Mediterranean Sea). *Mar. Chem.* 82, 161–183. doi:10.1016/S0304-4203(03)00051-3

Tolosa, I., LeBlond, N., Marty, J.-C., de Mora, S., and Prieur, L. (2005). Export fluxes of organic carbon and lipid biomarkers from the frontal structure of the Alboran Sea (SW Mediterranean Sea) in winter. *J. Sea Res.* 54, 125–142. doi:10.1016/J.SEARES.2005.04.002

Triantaphyllou, M. V. (2004). Coccolithophore export production and response to seasonal surface water variability in the oligotrophic Cretan Sea (NE Mediterranean). *Micropaleontology* 50, 127–144. doi:10.2113/50.Suppl_1.127

Tsapakis, M., Apostolaki, M., Eisenreich, S., and Stephanou, E. G. (2006). Atmospheric deposition and marine sedimentation fluxes of polycyclic aromatic hydrocarbons in the eastern Mediterranean basin. *Environ. Sci. Technol.* 40, 4922–4927. doi:10.1021/es060487x

Turchetto, M., Boldrin, A., Langone, L., and Miserocchi, S. (2012). Physical and biogeochemical processes controlling particle fluxes variability and carbon export in the Southern Adriatic. *Continent. Shelf Res.* 44, 72–82. doi:10.1016/j.csr.2011.05.005

Turner, J. T. (2015). Zooplankton fecal pellets, marine snow, phytodetritus and the ocean's biological pump. *Prog. Oceanogr.* 130, 205–248. doi:10.1016/J.POCEAN.2014.08.005

van der Jagt, H., Friese, C., Stuut, J.-B. W., Fischer, G., and Iversen, M. H. (2018). The ballasting effect of Saharan dust deposition on aggregate dynamics and carbon export: aggregation, settling, and scavenging potential of marine snow. *Limnol. Oceanogr.* 63, 1386–1394. doi:10.1002/lno.10779

Van Santvoort, P. J. M., de Lange, G. J., Thomson, J., Cussen, H., Wilson, T. R. S., Krom, M. D., et al. (1996). Active post-depositional oxidation of the most recent sapropel (S1) in sediments of the Eastern Mediterranean Sea. *Geochem. Cosmochim. Acta* 60, 4007–4024. doi:10.1016/S0016-7037(96)00253-0

Varkitzi, I., Psarra, S., Assimakopoulou, G., Pavlidou, A., Krasakopoulou, E., Velaoras, D., et al. (2020). Phytoplankton dynamics and bloom formation in the oligotrophic eastern mediterranean: field studies in the Aegean, Levantine and ionian seas. *Deep. Res. Part II Top. Stud. Oceanogr.* 171, 104662. doi:10.1016/j.dsr2.2019.104662

Versteegh, G. J., Bosch, H.-J., and De Leeuw, J. W. (1997). Potential palaeoenvironmental information of C_{24} to C_{36} mid-chain diols, keto-ols and mid-chain hydroxy fatty acids; a critical review. *Org. Geochem.* 27, 1–13. doi:1016/S0146-6380(97)00063-6

Versteegh, G. J. M., Jansen, J. H. F., Schneider, R. R., and De Leeuw, J. W. (2000). Mid-chain diols and keto-ols in SE atlantic sediments: a new tool for tracing past sea surface water masses?. *Geochem. Cosmochim. Acta* 64, 1879–1892. doi:10.1016/S0016-7037(99)00398-1

Versteegh, G. J. M., and Lipp, J. (2019). Detection of new long-chain mid-chain keto-ol isomers from marine sediments by means of HPLC–APCI-MS and comparison with long-chain mid-chain diols from the same samples. *Org. Geochem.* 133, 92–102. doi:10.1016/j.orggeochem.2019.04.004

Volk, T., and Hoffert, M. I. (1985). "Ocean carbon pumps: analysis of relative strengths and efficiencies in ocean-driven atmospheric CO_2 changes," in *The carbon cycle and atmospheric CO_2: natural variations Archean to present*. New York, NY: American Geophysical Union, 99–110. doi:10.1029/GM032p0099

Volkman, J. K. (1986). A review of sterol markers for marine and terrigenous organic matter. *Org. Geochem.* 9, 83–99. doi:10.1016/0146-6380(86)90089-6

Volkman, J. K., Barrett, S. M., and Blackburn, S. I. (1999). Eustigmatophyte microalgae are potential sources of C29 sterols, C22–C28 n-alcohols and C28–C32 n-alkyl diols in freshwater environments. *Org. Geochem.* 30, 307–318. doi:10.1016/S0146-6380(99)00009-1

Volkman, J. K., Barrett, S. M., Blackburn, S. I., Mansour, M. P., Sikes, E. L., and Gelin, F. (1998). Microalgal biomarkers: a review of recent research developments. *Org. Geochem.* 14, 1163–1179. doi:10.1016/S0146-6380(98)00062-X

Volkman, J. K., Barrett, S. M., Dunstan, G. A., and Jeffrey, S. W. (1992). C_{30} C_{32} alkyl diols and unsaturated alcohols in microalgae of the class Eustigmatophyceae. *Org. Geochem.* 18, 131–138. doi:10.1016/0146-6380(92)90150-V

Volkman, J. K. (2006). "Lipid markers for marine organic matter," in *Marine organic matter: biomarkers, isotopes and DNA*. Editor J. K. Volkman (Berlin: Springer-Verlag), 27–70.

Volkman, J. K., and Tanoue, E. (2002). Chemical and biological studies of particulate organic matter in the ocean. *J. Oceanogr.* 58, 265–279. doi:10.1023/A:1015809708632

Wakeham, S. G., Canuel, E. A., Lerberg, E. J., Mason, P., Sampere, T. P., and Bianchi, T. S. (2009). Partitioning of organic matter in continental margin sediments among density fractions. *Mar. Chem.* 115, 211–225. doi:10.1016/j.marchem.2009.08.005

Wakeham, S. G., and Canuel, E. A. (1986). Lipid composition of the pelagic crab *Pleuroncodes planipes*, its feces, and sinking particulate organic matter in the Equatorial North Pacific Ocean. *Org. Geochem.* 9, 331–343. doi:10.1016/0146-6380(86)90114-2

Wakeham, S. G. (1995). Lipid biomarkers for heterotrophic alteration of suspended particulate organic matter in oxygenated and anoxic water columns of the ocean. *Deep-Sea Res. Part I Oceanogr. Res. Pap.* 42, 1749–1771. doi:10.1016/0967-0637(95)00074-G

Wakeham, S. G., Peterson, M. L., Hedges, J. I., and Lee, C. (2002). Lipid biomarker fluxes in the Arabian sea, with a comparison to the equatorial pacific ocean. *Deep Sea Res. Part II Top. Stud. Oceanogr.* 49, 2265–2301. doi:10.1016/S0967-0645(02)00037-1

Wang, Z., Fingas, M., and Page, D. S. (1999). Oil spill identification. *J. Chromatogr. A* 843, 369–411. doi:10.1016/S0021-9673(99)00120-X

Warnken, C. (2003). Biogeochemie von Schwebstoffen, Sinkstoffen und Sedimenten im Ierapetra-Tief (östliches Mittelmeer). Diploma thesis. Inst. für Biogeochem. und Meereschem. Hamburg: University of Hamburg.

Weinbauer, M. G., Guinot, B., Migon, C., Malfatti, F., and Mari, X. (2017). Skyfall—neglected roles of volcano ash and black carbon rich aerosols for microbial plankton in the ocean. *J. Plankton Res.* 39, 187–198. doi:10.1093/plankt/fbw100

Yunker, M. B., Macdonald, R. W., Veltkamp, D. J., and Cretney, W. J. (1995). Terrestrial and marine biomarkers in a seasonally ice-covered Arctic estuary — integration of multivariate and biomarker approaches. *Mar. Chem.* 49, 1–50. doi:10.1016/0304-4203(94)00057-K

Ziveri, P., Rutten, A., de Lange, G. J., Thomson, J., and Corselli, C. (2000). Present-day coccolith fluxes recorded in central eastern Mediterranean sediment traps and surface sediments. *Palaeogeogr. Palaeoclimatol. Palaeoecol.* 158, 175–195. doi:10.1016/S0031-0182(00)00049-3

Zúñiga, D., Flexas, M. M., Sanchez-Vidal, A., Coenjaerts, J., Calafat, A., Jordà, G., et al. (2009). Particle fluxes dynamics in Blanes submarine canyon (Northwestern Mediterranean). *Prog. Oceanogr.* 82, 239–251. doi:10.1016/j.pocean.2009.07.002

Conflict of Interest: The authors declare that the research was conducted in the absence of any commercial or financial relationships that could be construed as a potential conflict of interest.